The QUIJOTE experiment and the study of the polarization of the CMB

Ricardo Génova Santos
for the QUIJOTE collaboration
rgs@iac.es

XV Christmas Workshop, Instituto de Física Teórica (UAM)
Madrid, 16-18 December 2009

Outline

❖ Introduction. The cosmic microwave background (CMB)
- Inflation and the early Universe
- Observations of the temperature fluctuations in the CMB. Past (VSA, ACBAR, CBI,...), present (WMAP, ...) and future (Planck,...) experiments

❖ The study of the polarization of the CMB
- E-modes and B-modes
- The gravitational wave background
- Prospects for its detection and contaminants
- Projected experiments (QUIET, SPIDER, EBEX,...)

❖ The QUIJOTE-CMB experiment
- Location and experimental setup. Telescope and instrument
- Science goals
- Current status and future plans

Introduction. The Cosmic Microwave Background

Thermal history of the Universe

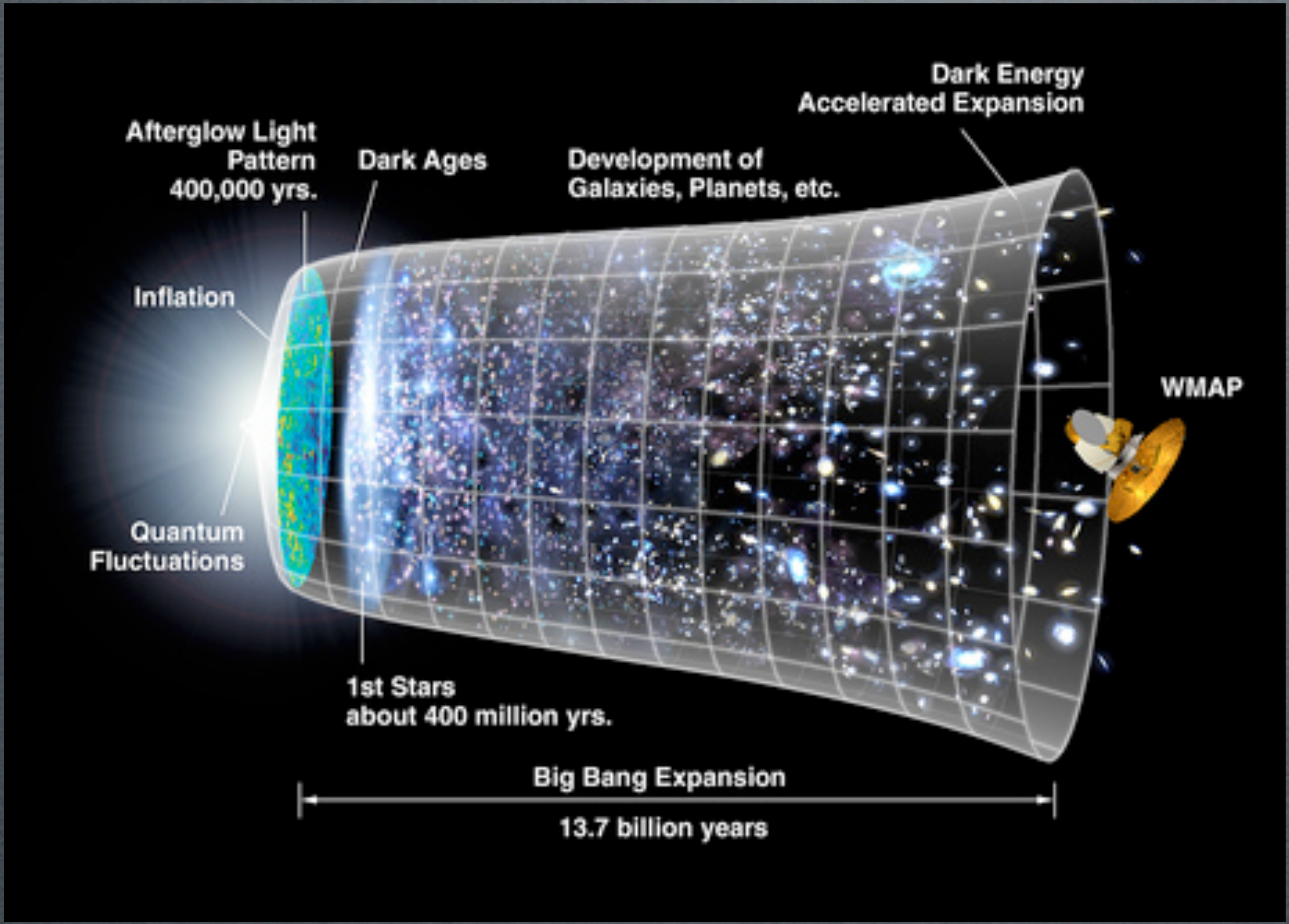

- Big Bang
- $t \approx 10^{-36}$ s, $T > 10^{12}$ K: inflation
- $t \approx 1$ s, $T \approx 10^{10}$ K: neutrino/antineutrino decoupling
- $t \approx 14$ s, $T \approx 10^{9}$ K: electrons and positrons annihilation
- $t \approx 3$ min: primordial nucleosynthesis (BBN)
- $t \approx 380{,}000$ yr, $T \approx 3000$K: recombination
- Decoupling $\Rightarrow$ CMB

The Cosmic Microwave Background

❖ Gamow (1946) proposed the Big Bang model to explain the primordial nucleosynthesis

❖ Alpher & Herman (1948) suggested that the Universe should have a ~5K temperature, from which a radiation background would be expected ⇒ the Cosmic Microwave Background

❖ First observed by A. Penzias and R. Wilson in 1964, as an excess of noise at λ=5.3 cm using a Bell Telephone horn antenna in Holmdel (New Jersey). Both were awarded with the Physics Nobel Prize in 1978

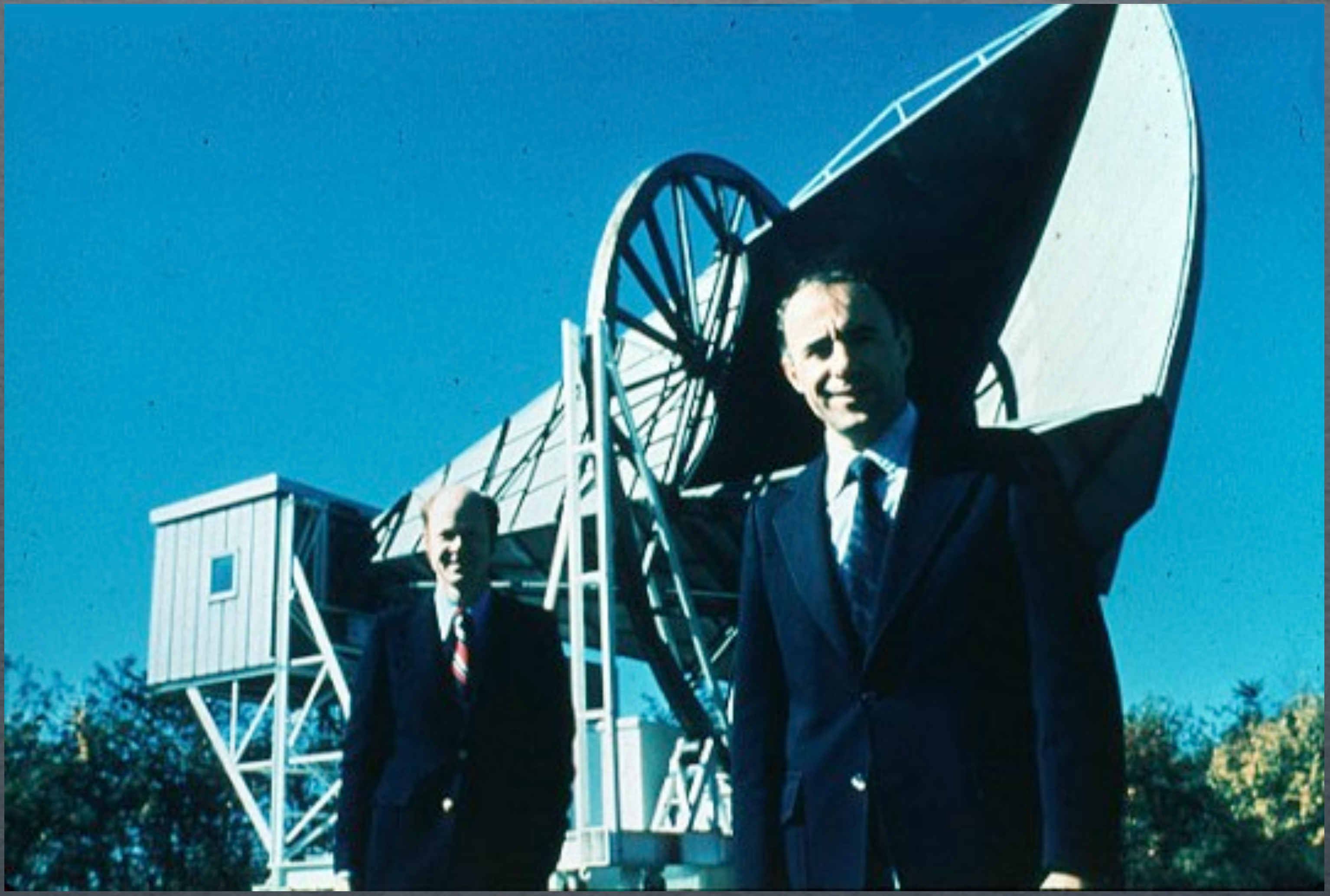

The Cosmic Microwave Background

❖ NASA COsmic Background Observer (COBE) satellite. Launched in 1989

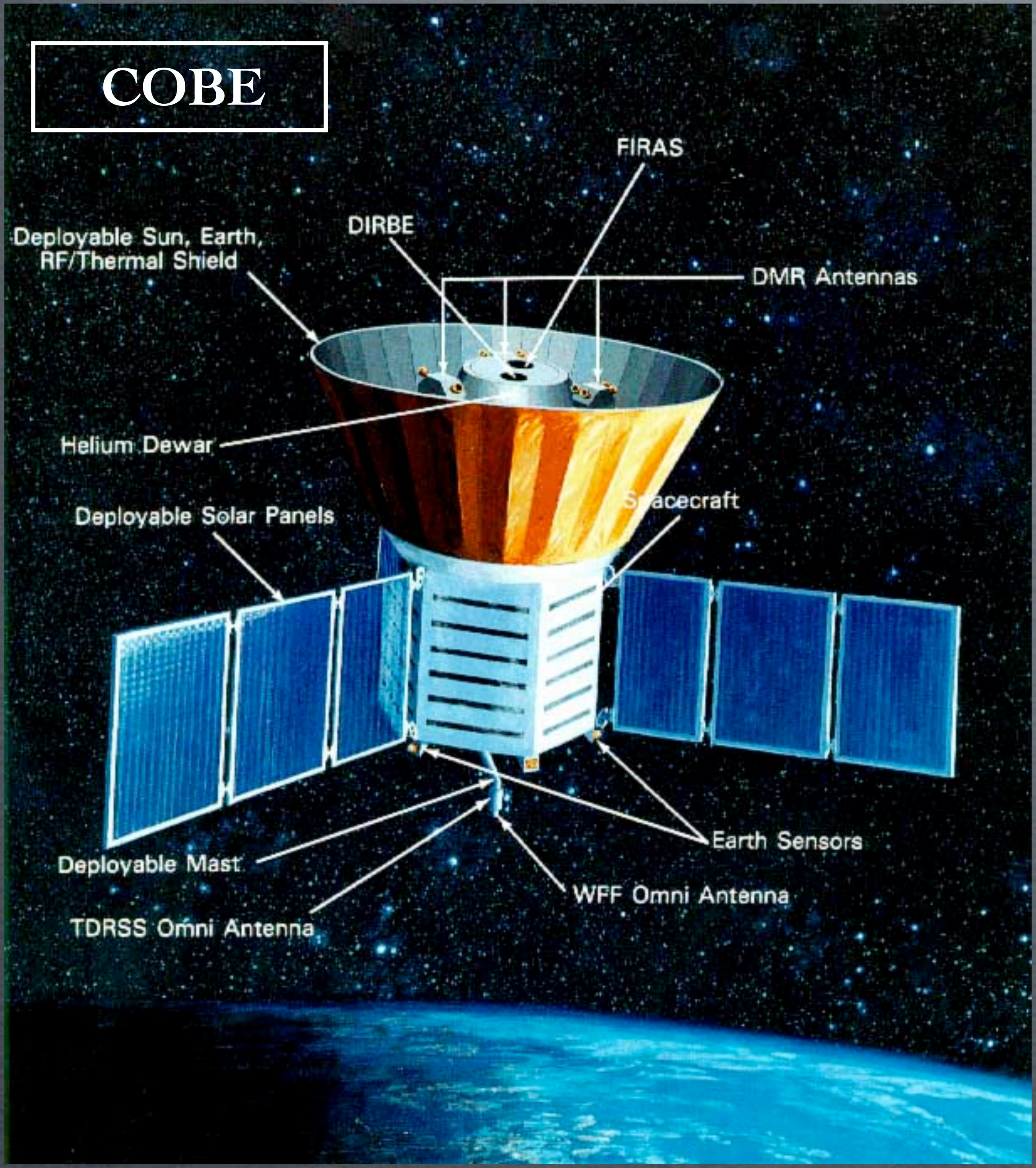

❖ Far InfraRed Absolute Spectrophotometer (FIRAS) determined:

- Perfect Planck-type spectrum, with $T_0 = 2.728 \pm 0.004$ K (Fixsen et al. 1996)

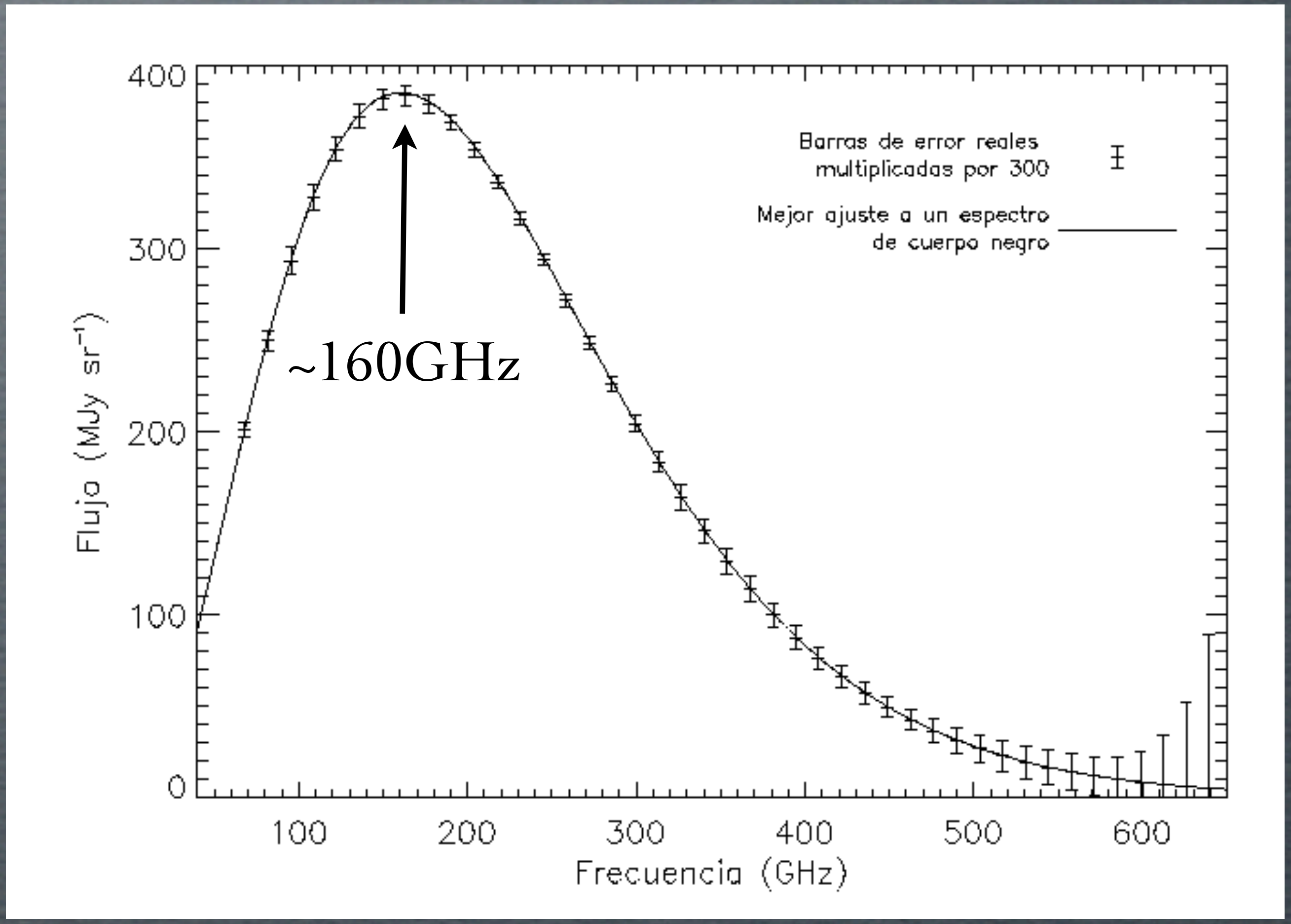

The Cosmic Microwave Background

❖ Differential Microwave Radiometer (DMR) determined (Bennett et al. 1996):

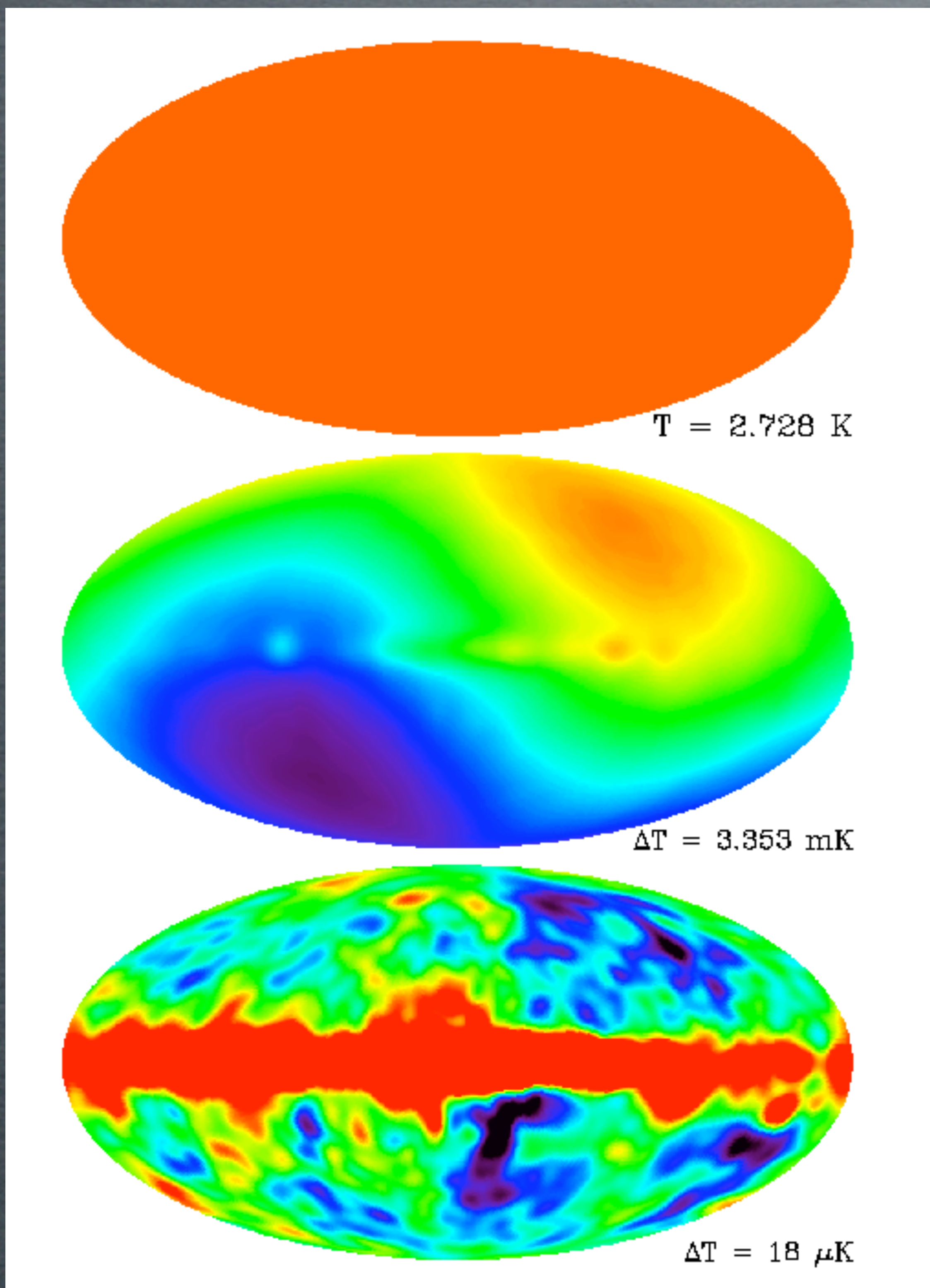

All-sky isotropic radiation (monopole), with $T_0 = 2.725 \pm 0.020$ K

Large-scale anisotropy, $\Delta T/T_0 \sim 10^{-3}$, with amplitude $\Delta T \sim 3.353 \pm 0.024$ K (dipole)

Temperature fluctuations in ~7° angular scales, of the order $\Delta T/T_0 \sim 10^{-5} \Rightarrow$ CMB primary anisotropies

Physics Nobel Prize 2006 winners

John C. Mather (FIRAS PI)

George F. Smoot (DMR PI)

CMB primary anisotropies

❖ Baryon-photon plasma before recombination

❖ The fluctuations in the intensity of the CMB are a consequence of the variation in the distribution of matter in the epoch of recombination

❖ Observations of these anisotropies are crucial because they yield information about the matter distribution when the Universe was only 380,000 years old

❖ Contaminants:

- Secondary anisotropies:
  - Sunyaev-Zel'dovich (SZ) effect
  - Integrated Sachs-Wolfe (ISW) effect
  - Rees-Sciama (RS) effect
  - Ostriker-Vishniac (OS) effect
  - Reionization (global, patchy)
  - Lensing
- Emission mechanisms in microwaves:
  - Galactic contaminants (synchrotron, free-free, thermal dust emission)
  - Extragalactic point-sources
  - Atmosphere

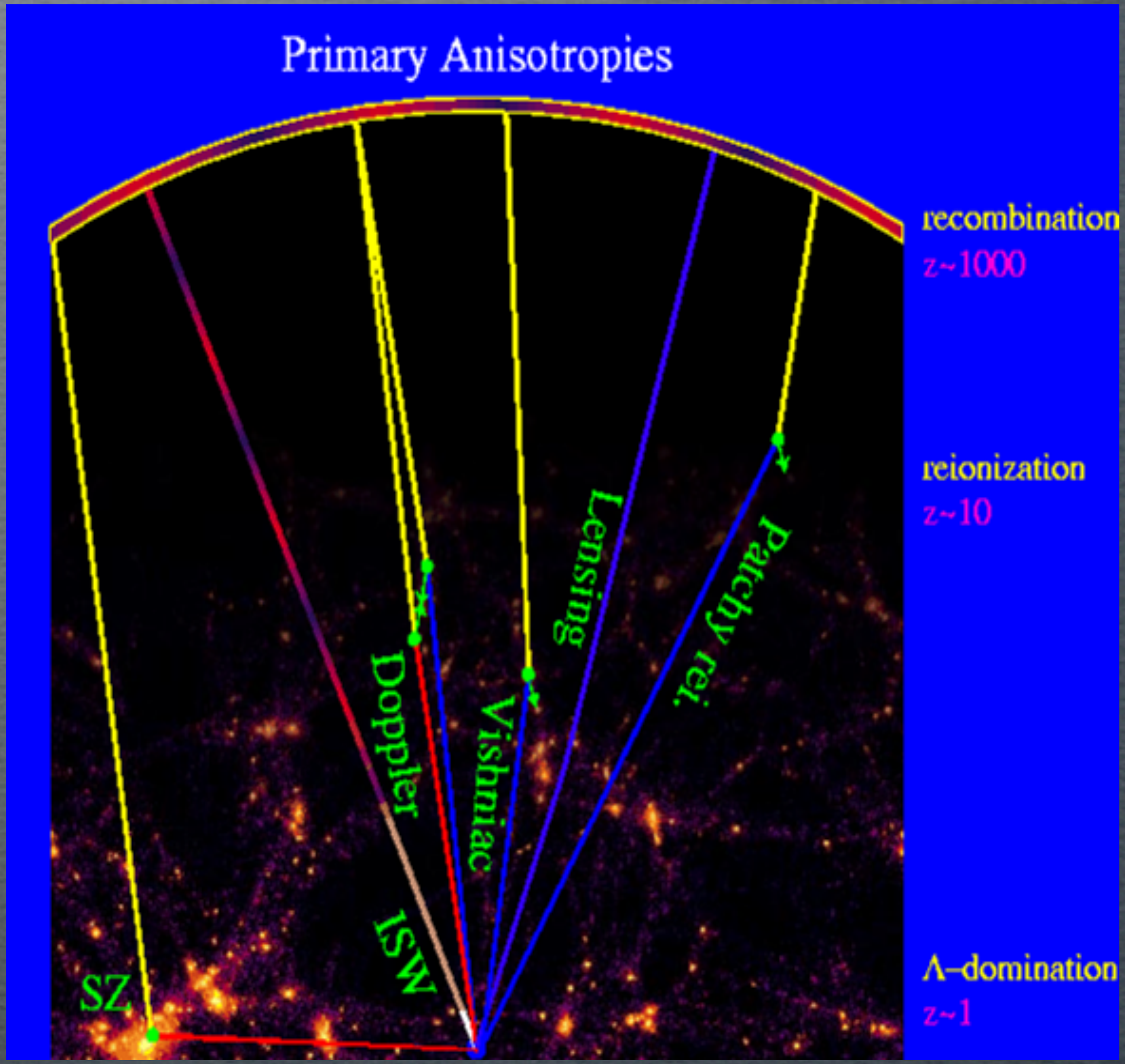

The angular power spectrum

- Spherical harmonic decomposition over the sphere of the temperature fluctuations

$$\frac{\Delta T}{T_0}(\theta,\phi) = \sum_{\ell=2}^{\infty}\sum_{m=-\ell}^{\ell} a_{\ell m} Y_{\ell m}(\theta,\phi)$$

- The a_{lm} coefficients are random and independent variables with zero mean

$$C_\ell = \frac{1}{2\ell+1}\sum_{m=-\ell}^{\ell} a_{\ell m} a^*_{\ell m} = \langle |a_{\ell m}|^2 \rangle$$

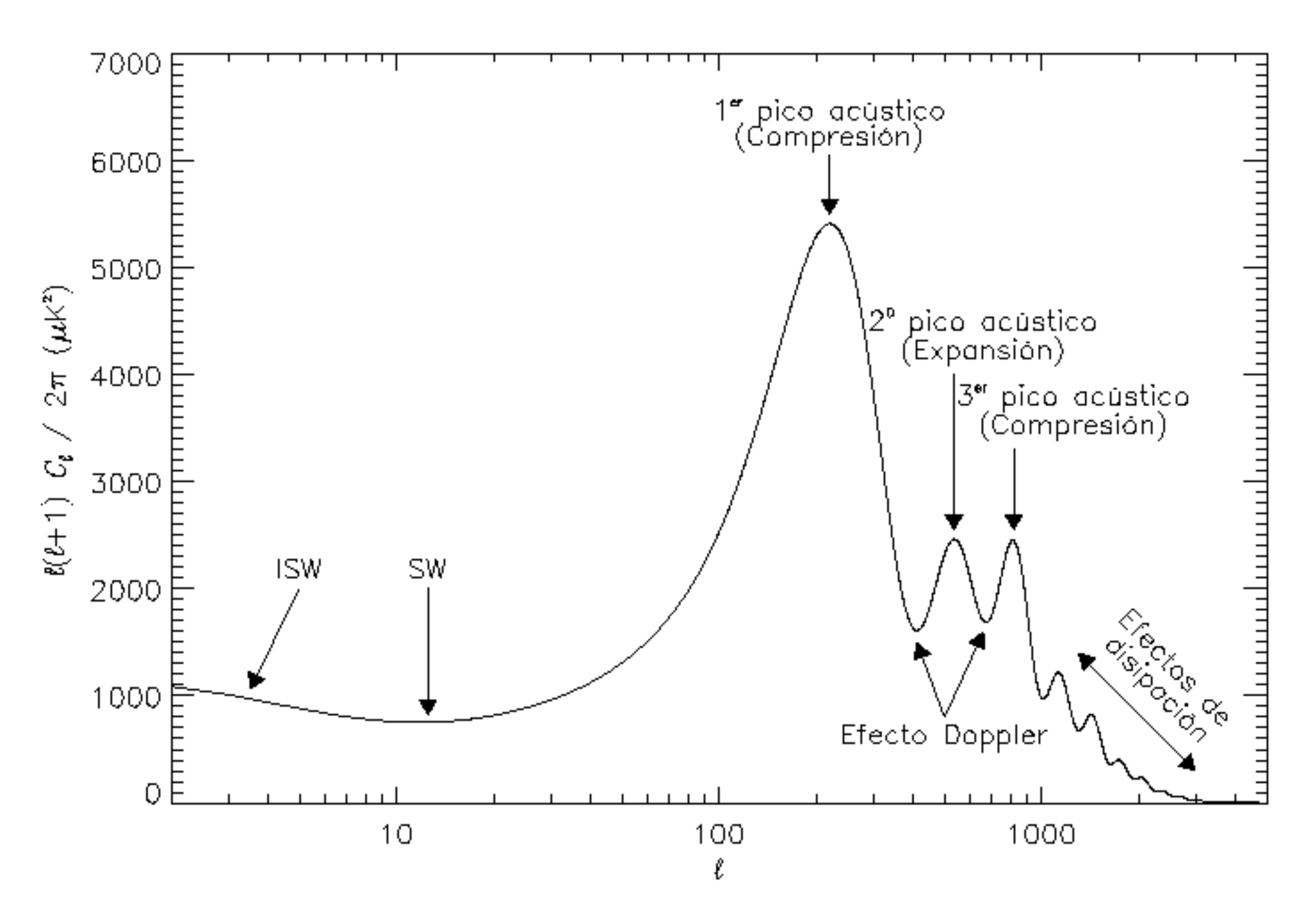

Power spectrum of the temperature fluctuations.

- It represents the power associated to each multipole l
- It encodes all the statistical information of the CMB fluctuations
- In the real space it is the two-point correlation function

$$C(\theta) = \left\langle \frac{\Delta T}{T_0}(\hat{n}_1)\frac{\Delta T}{T_0}(\hat{n}_2)\right\rangle = \frac{1}{4\pi}\sum_{\ell=2}^{\infty}\sum_{m=-\ell}^{\ell}|a_{\ell m}|^2 P_\ell(\cos\theta) = \frac{1}{4\pi}\sum_{\ell=2}^{\infty}(2\ell+1)C_\ell P_\ell(\cos\theta)$$

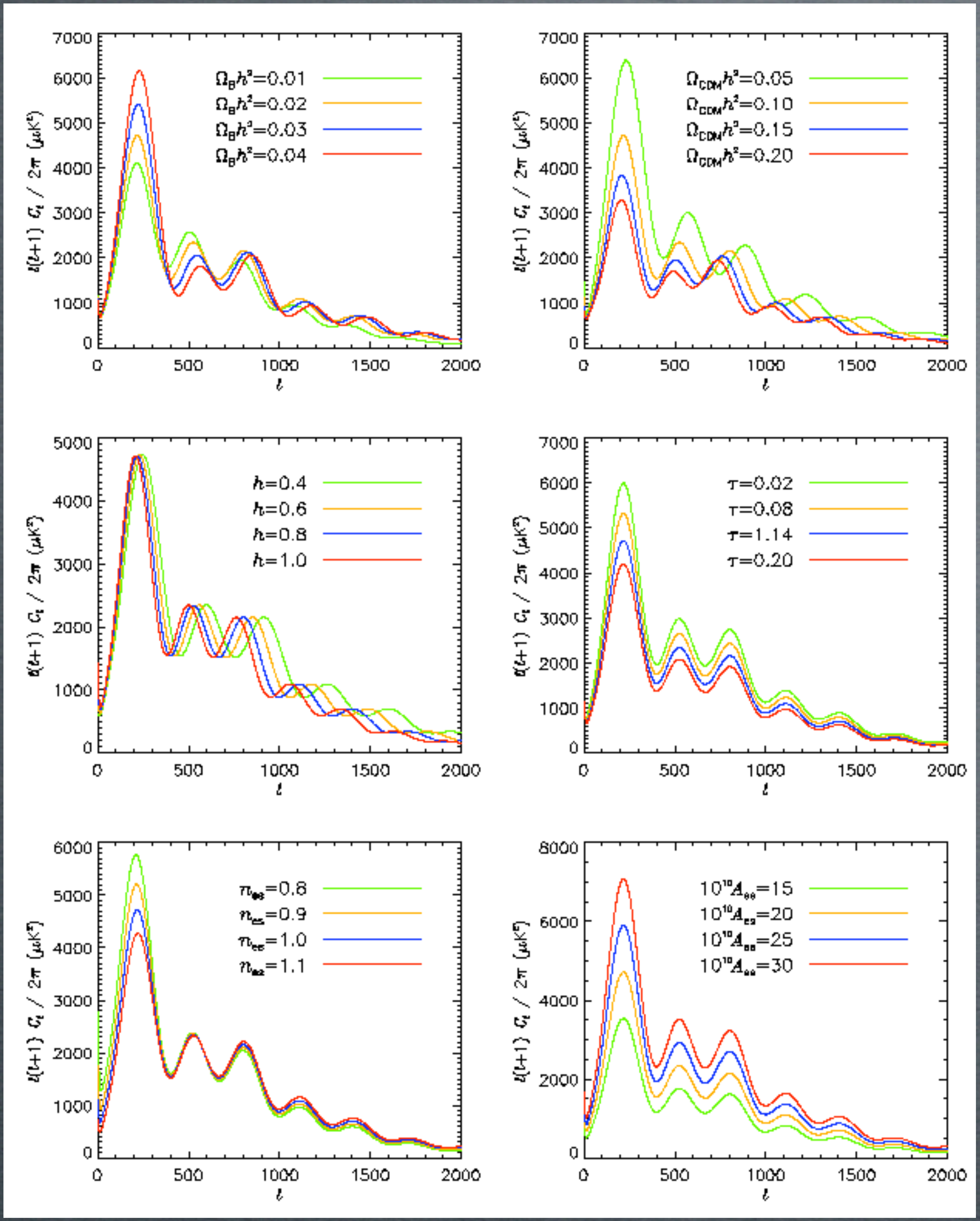

❖ The positions and heights of the peaks depend upon the most important cosmological parameters

- The position of the first peak is sensitive to the geometry of the Universe (Ω_{tot})
- The high-l peaks heights yield information about the LSS width and the reionization
- The relative heights of the peaks change with $\Omega_B h^2$ and n_s
- The positions of the second and higher-order peaks change with $\Omega_{CDM} h^2$, $\Omega_B h^2$ and h

Observations of the CMB anisotropies

❖ Several experiments were designed in the last ~10 years to measure the CMB primary anisotropies power spectrum

Experimento	Tipo	ν (GHz)	FWHM	Cobertura multipolar
COBE	S.E. / 6 Rad.	31.5, 53, y 90	$\sim 7°$	$\ell = 0, 1, 2$ (Bennett et al., 1996) $3 \leq \ell \lesssim 30$ (Wright et al., 1996)
Tenerife	T. / 3 Rad.	10, 15 y 33	$\approx 5°$	$10 \lesssim \ell \lesssim 30$ (Gutiérrez et al., 2000)
BOOMERANG	G.E. / 16 Bol.	90, 150 240 y 410 [a]	$\approx$ 18, 10, 14 y 12' [a]	$50 \leq \ell \leq 600$ (de Bernardis et al., 2000) $75 \leq \ell \leq 1025$ (Netterfield et al., 2002) $50 \leq \ell \leq 1500$ (Jones et al., 2006)
MAXIMA	G.E. / 16 Bol.	150, 240 y 410	10'	$36 \leq \ell \leq 785$ (Hanany et al., 2000) $36 \leq \ell \leq 1235$ (Lee et al., 2001)
DASI	T. / Int. 13 Ant.	26-36	$\approx$20'	$100 < \ell < 900$ (Halverson et al., 2002)
ARCHEOPS	G.E. / 21 Bol.	143, 217, 353 y 545	$\sim$12'	$15 < \ell < 350$ (Benoît et al., 2003a) $10 < \ell < 700$ (Tristram et al., 2005)
WMAP	S.E. / 20 Rad.	23, 33, 41, 61 y 94	53, 40, 31, 21 y 13'	$2 \leq \ell \lesssim 700$ (Hinshaw et al., 2003) $2 \leq \ell \lesssim 850$(Hinshaw et al., 2006)
CBI	T. / Int. 13 Ant.	26-36	4.5-8'	$200 < \ell < 3500$ (Mason et al., 2003) $400 < \ell < 3500$ (Readhead et al., 2004)
ACBAR	T. / 16 Bol.	150, 220 y 280	4.8, 3.9 y 3.9'	$150 < \ell < 3000$ (Kuo et al., 2004)
PLANCK	S.E. / 56 Rad. + 48 Bol.	30, 44, 70, 100, 143, 217, 353, 545 y 857	33, 24, 14, 9.5, 7.1, 5.0, 5.0, 5.0 y 5.0'	$0 < \ell \lesssim 2000$ (su lanzamiento está previsto para 2007)

Observations of the CMB anisotropies

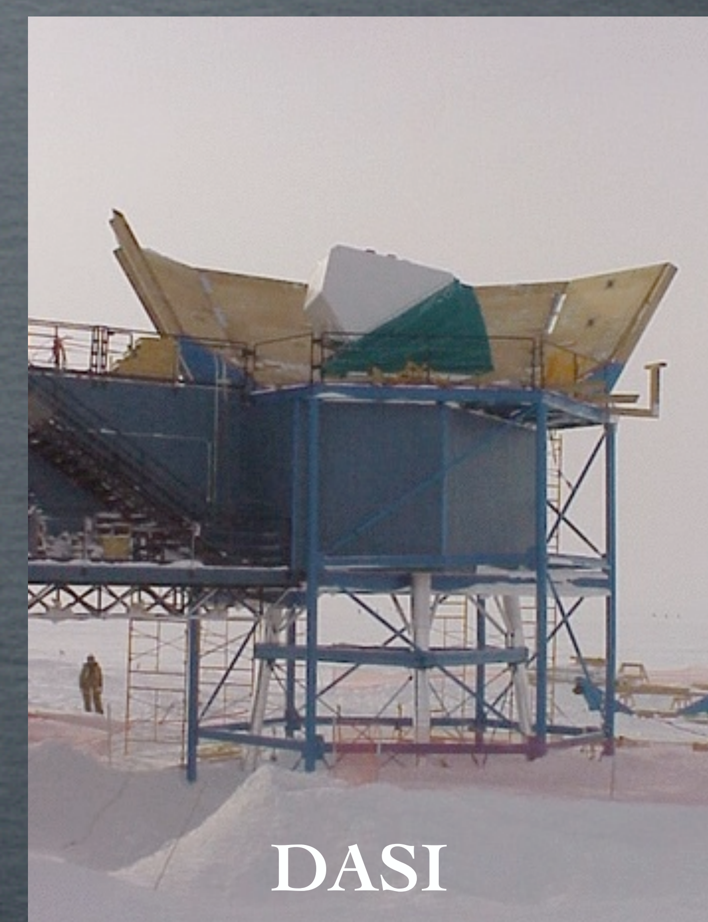

CMB studies at the Teide Observatory

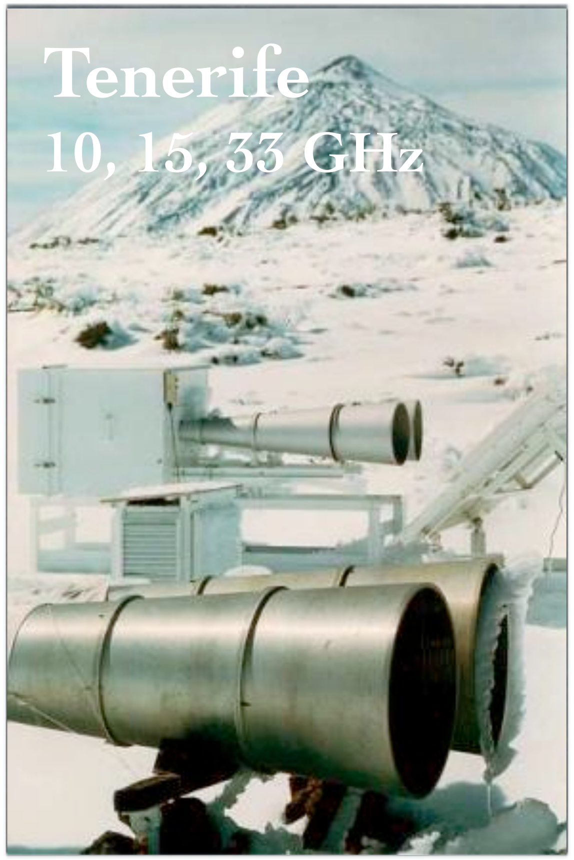

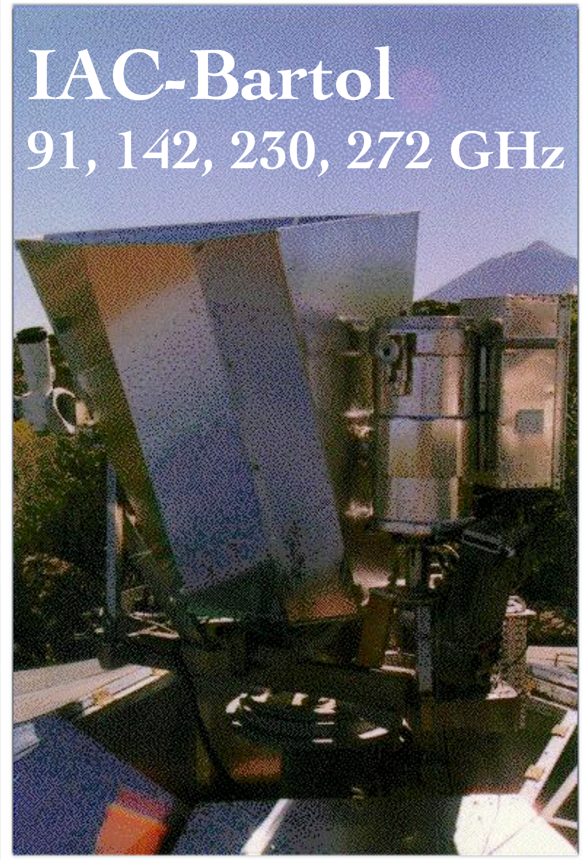

The Very Small Array

- 14-element interferometer at the Teide Observatory, operating at 33 GHz
- Collaboration: Cambridge, Manchester and the IAC
- It operated in three different configurations

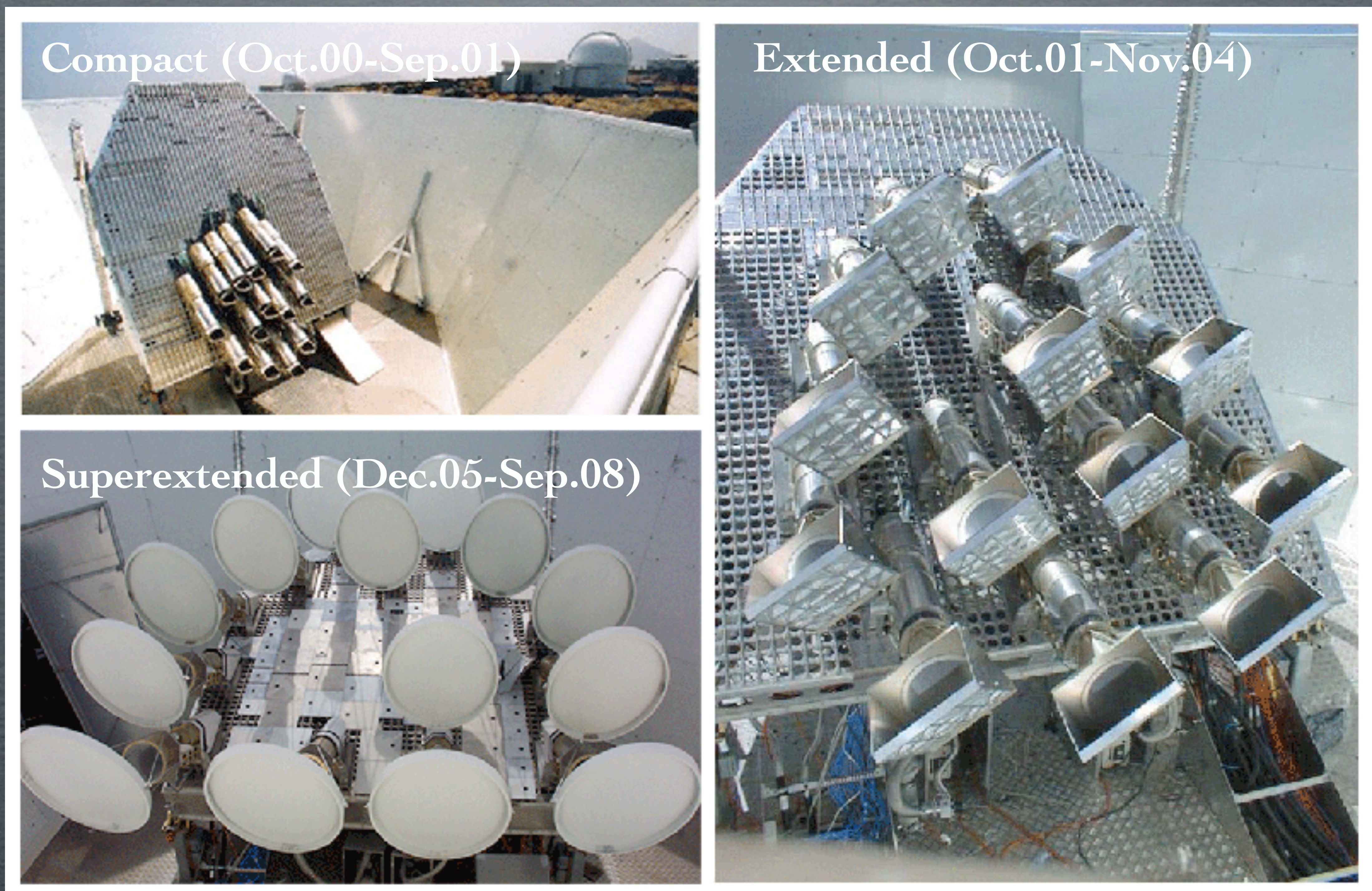

VSA maps of the primordial CMB

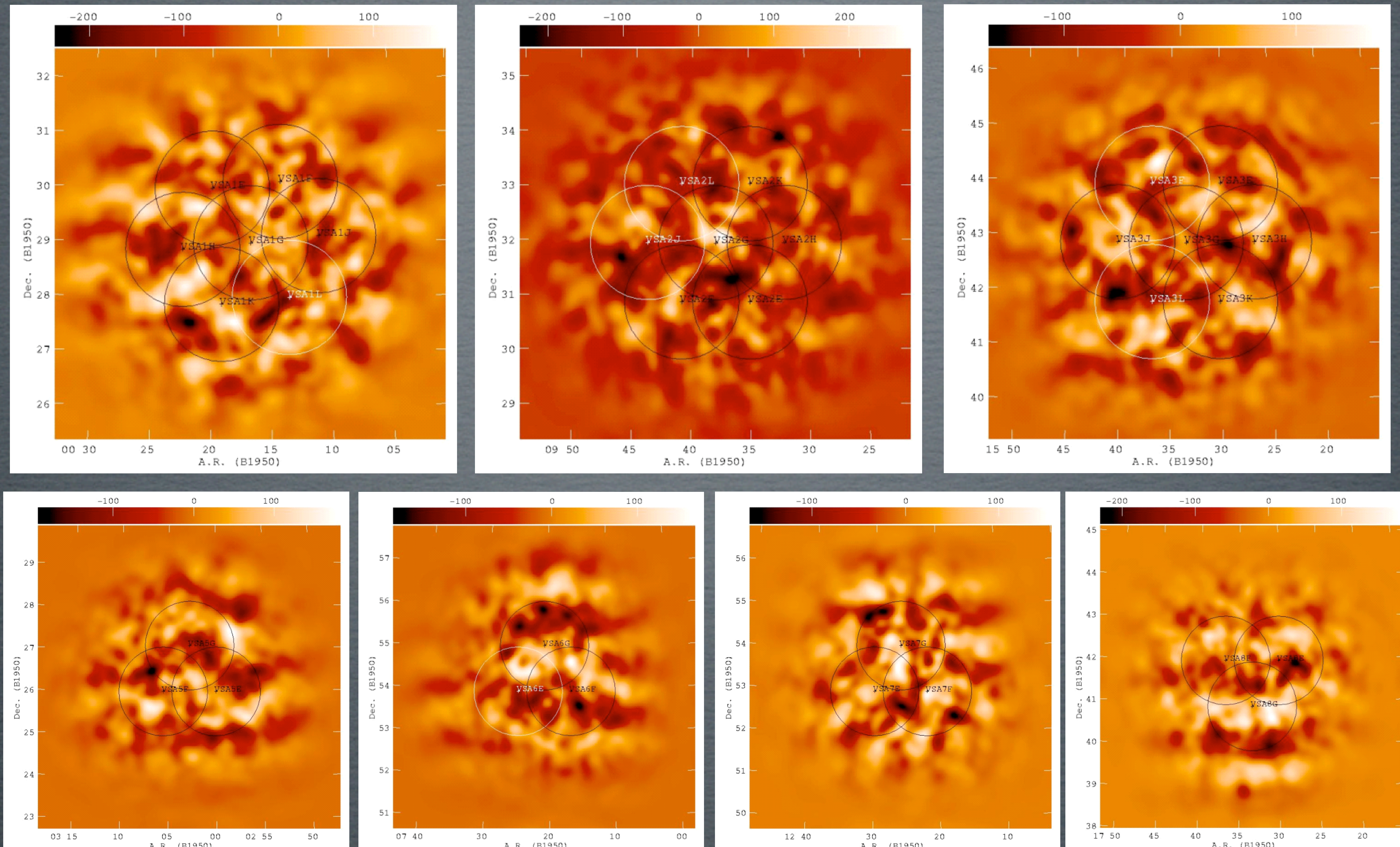

(Dickinson et al. 2004)

Wilkinson Microwave Anisotropy Probe (WMAP)

- NASA satellite launched on June 2001
- All-sky survey at 5 frequency bands: K (23 GHz), Ka (33), Q (41), V (61), W (94)
- Angular resolutions from 0.82 to 0.21 degrees

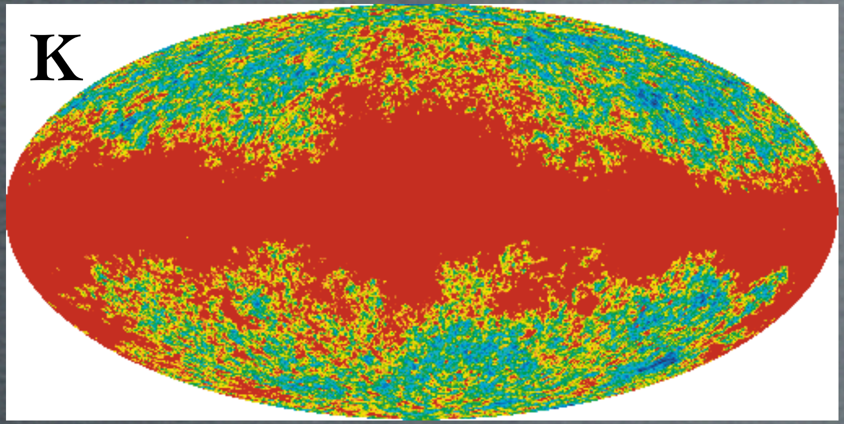

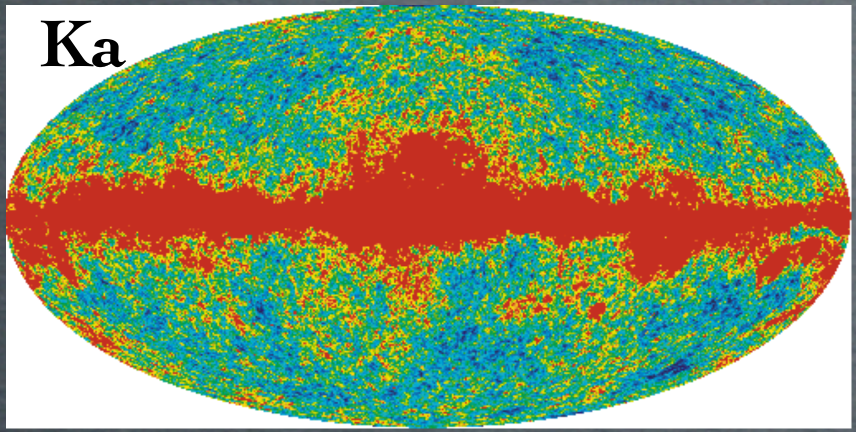

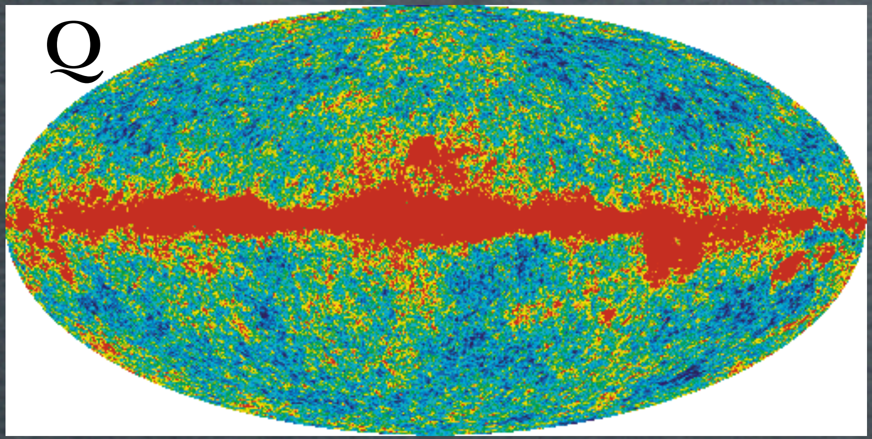

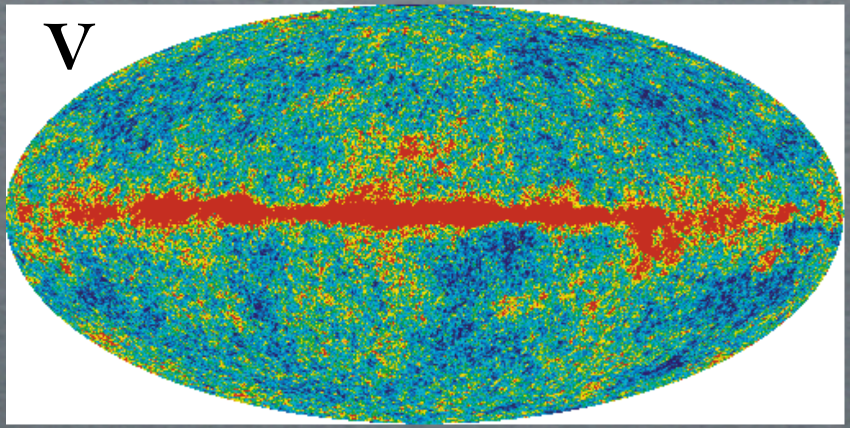

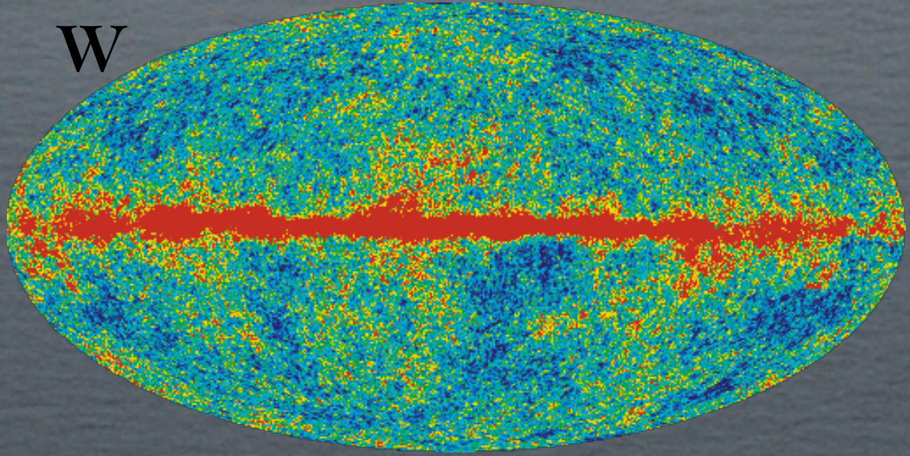

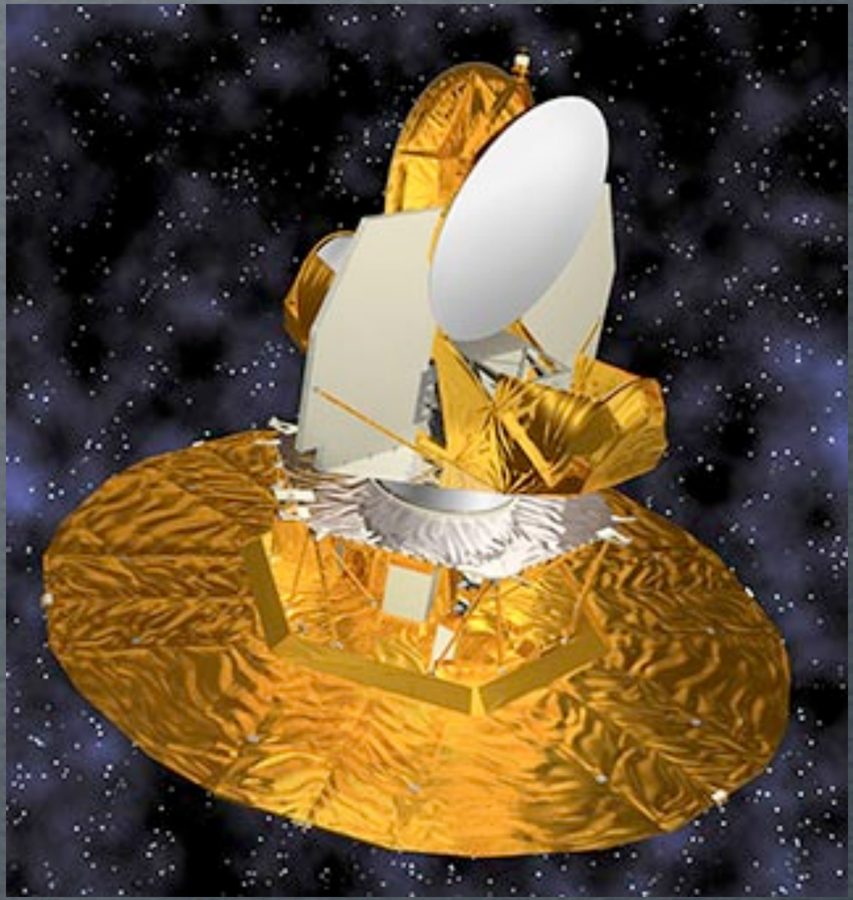

From COBE to WMAP

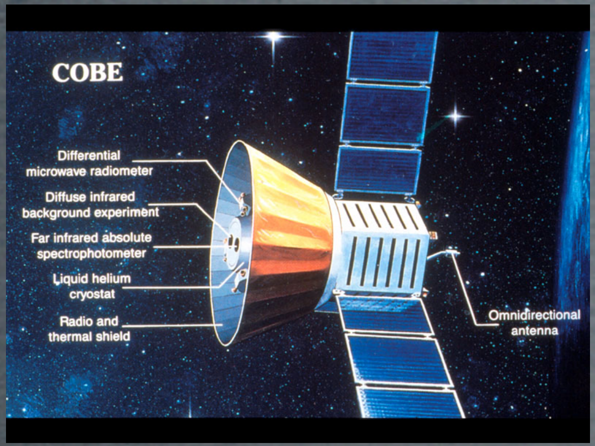

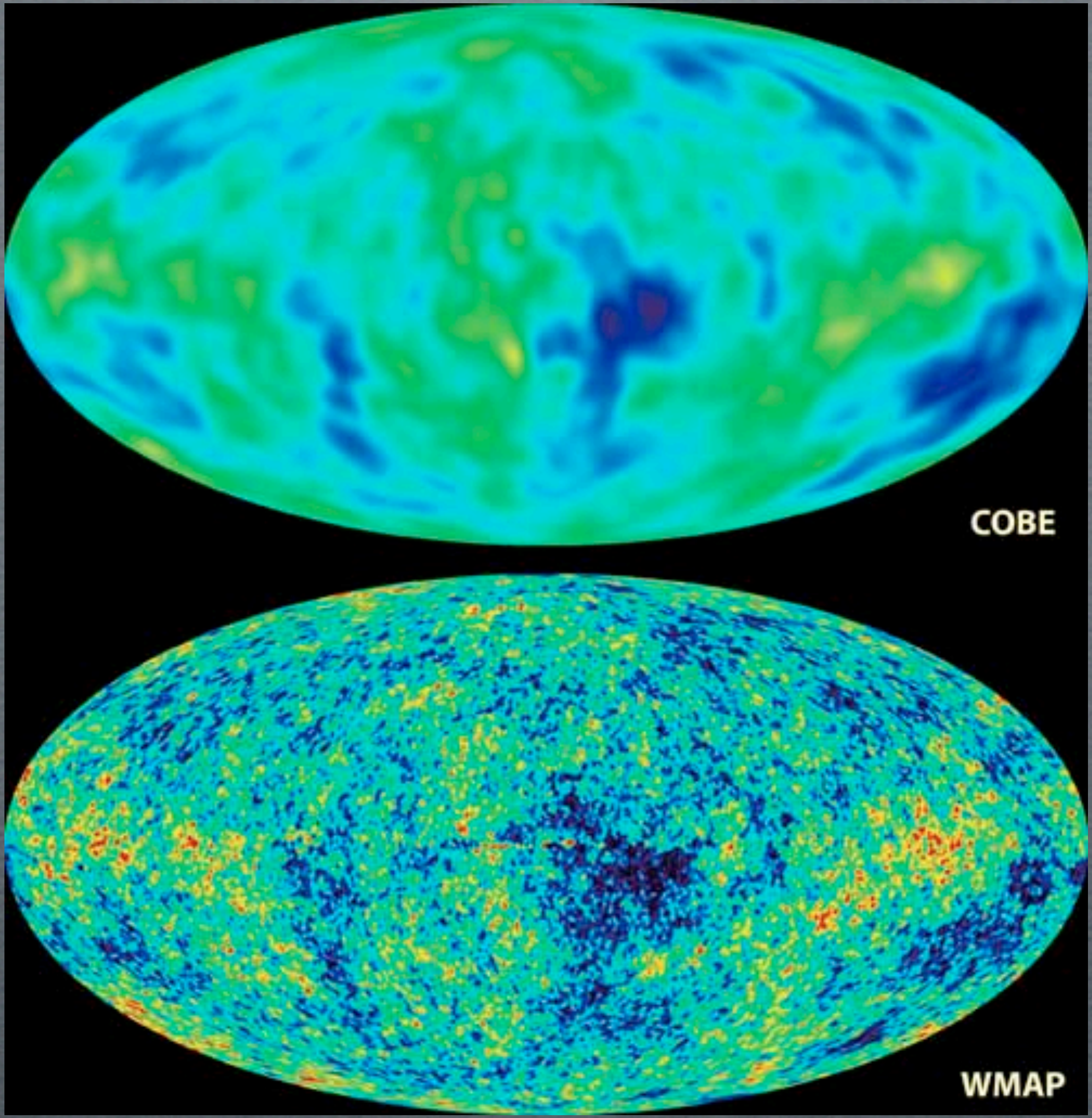

(1996)

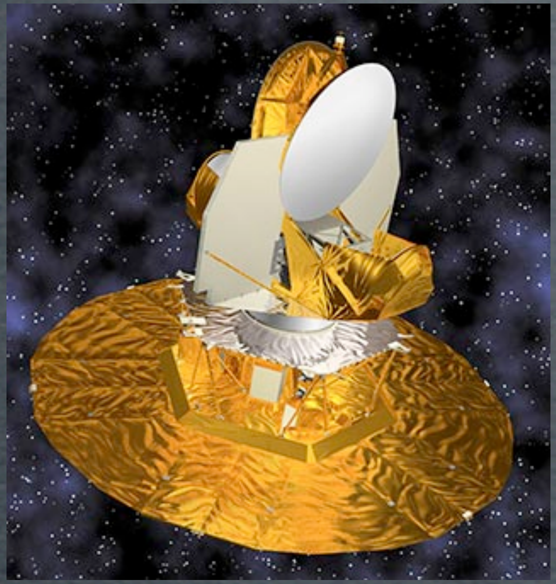

(2003)

Observations of the CMB anisotropies

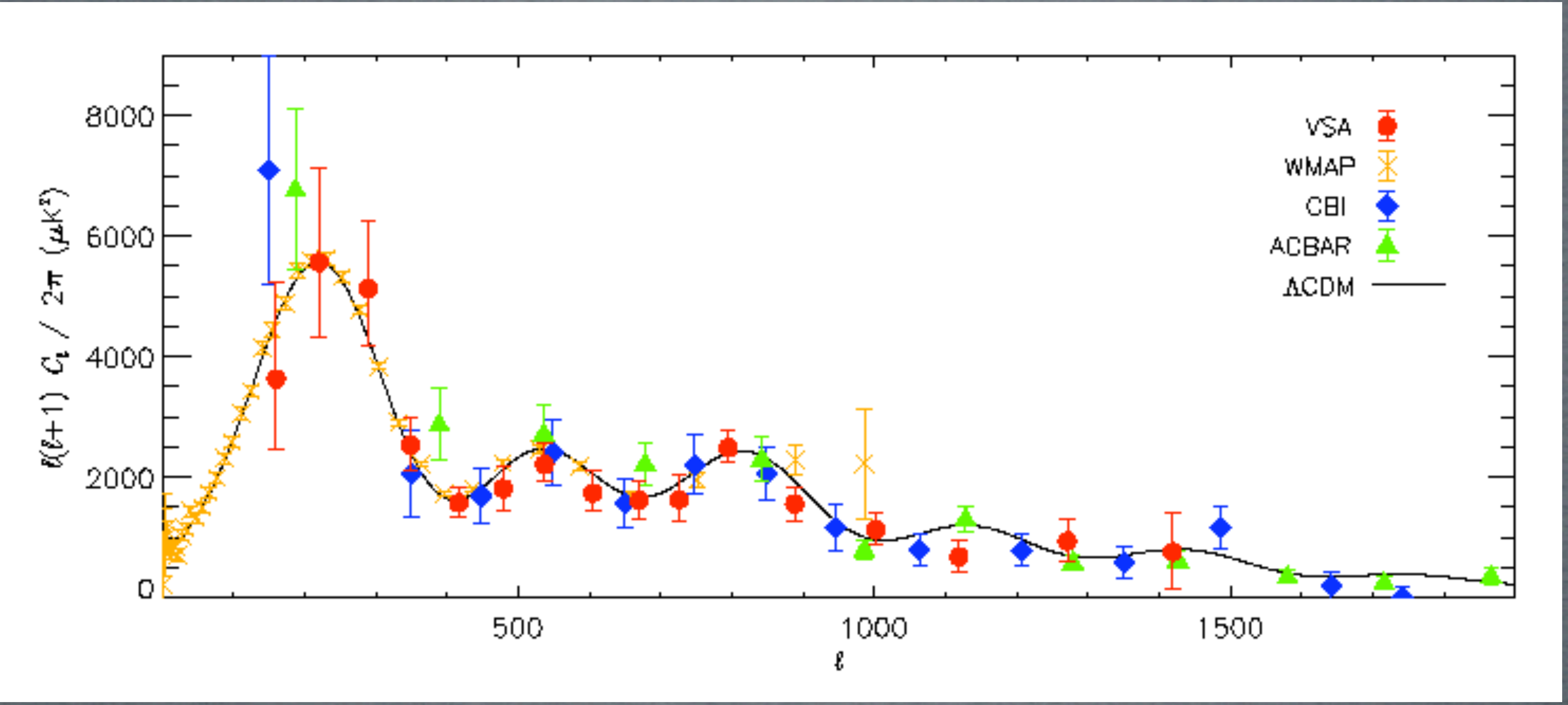

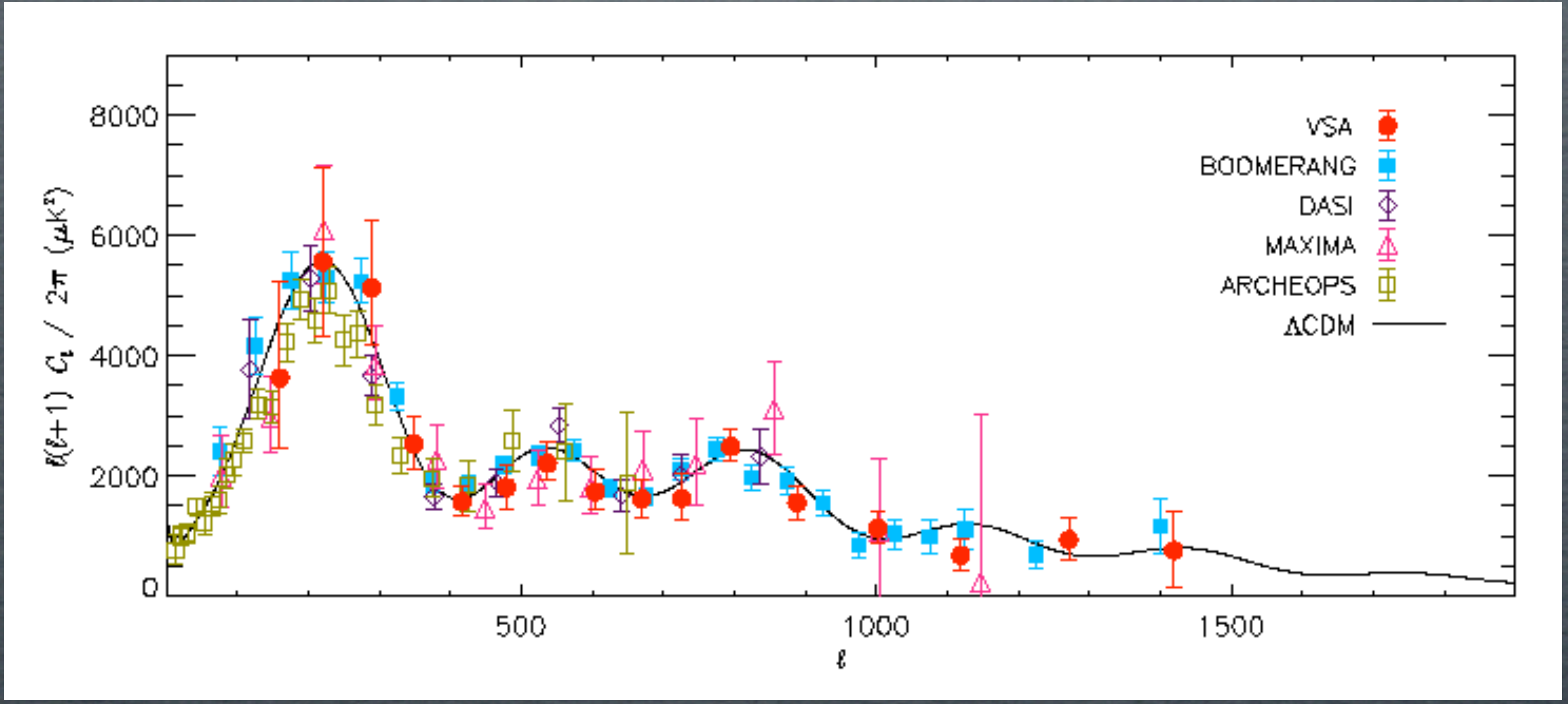

Cosmological parameters from WMAP

Description	Symbol	Value	+ Uncertainty	− Uncertainty
Total density	Ω_{tot}	1.02	0.02	0.02
Equation of state of quintessence	w	<-0.78	95% CL	...
Dark energy density	Ω_Λ	0.73	0.04	0.04
Baryon density	$\Omega_b h^2$	0.0224	0.0009	0.0009
Baryon density	Ω_b	0.044	0.004	0.004
Baryon density (cm^{-3})	n_b	2.5×10^{-7}	0.1×10^{-7}	0.1×10^{-7}
Matter density	$\Omega_m h^2$	0.135	0.008	0.009
Matter density	Ω_m	0.27	0.04	0.04
Light neutrino density	$\Omega_\nu h^2$	<0.0076	95% CL	...
CMB temperature (K)[a]	T_{CMB}	2.725	0.002	0.002
CMB photon density (cm^{-3})[b]	n_γ	410.4	0.9	0.9
Baryon-to-photon ratio	η	6.1×10^{-10}	0.3×10^{-10}	0.2×10^{-10}
Baryon-to-matter ratio	$\Omega_b \Omega_m^{-1}$	0.17	0.01	0.01
Fluctuation amplitude in 8 h^{-1} Mpc spheres	σ_8	0.84	0.04	0.04
Low-z cluster abundance scaling	$\sigma_8 \Omega_m^{0.5}$	0.44	0.04	0.05
Power spectrum normalization (at $k_0 = 0.05$ Mpc^{-1})[c]	A	0.833	0.086	0.083
Scalar spectral index (at $k_0 = 0.05$ Mpc^{-1})[c]	n_s	0.93	0.03	0.03
Running index slope (at $k_0 = 0.05$ Mpc^{-1})[c]	$dn_s/d\ln k$	−0.031	0.016	0.018
Tensor-to-scalar ratio (at $k_0 = 0.002$ Mpc^{-1})	r	<0.90	95% CL	...
Redshift of decoupling	z_{dec}	1089	1	1
Thickness of decoupling (FWHM)	Δz_{dec}	195	2	2
Hubble constant	h	0.71	0.04	0.03
Age of universe (Gyr)	t_0	13.7	0.2	0.2
Age at decoupling (kyr)	t_{dec}	379	8	7
Age at reionization (Myr, 95% CL)	t_r	180	220	80
Decoupling time interval (kyr)	Δt_{dec}	118	3	2
Redshift of matter-energy equality	z_{eq}	3233	194	210
Reionization optical depth	τ	0.17	0.04	0.04
Redshift of reionization (95% CL)	z_r	20	10	9
Sound horizon at decoupling (deg)	θ_A	0.598	0.002	0.002
Angular size distance (Gpc)	d_A	14.0	0.2	0.3
Acoustic scale[d]	ℓ_A	301	1	1
Sound horizon at decoupling (Mpc)[d]	r_s	147	2	2

Bennett et al. (2003)

- WMAP1
- COBE
- CBI
- ACBAR
- 2dFGRS

Planck

- ESA satellite launched on May 14, 2009
  - All-sky survey
  - Wide frequency coverage: Low Frequency Instrument (33, 44, 70 GHz) and High Frequency Instrument (100, 143, 217, 353, 545, 857 GHz)
  - Unprecedented angular resolution (33' to 5') and sensitivity
  - First Light Survey. 10% sky coverage. Recently published

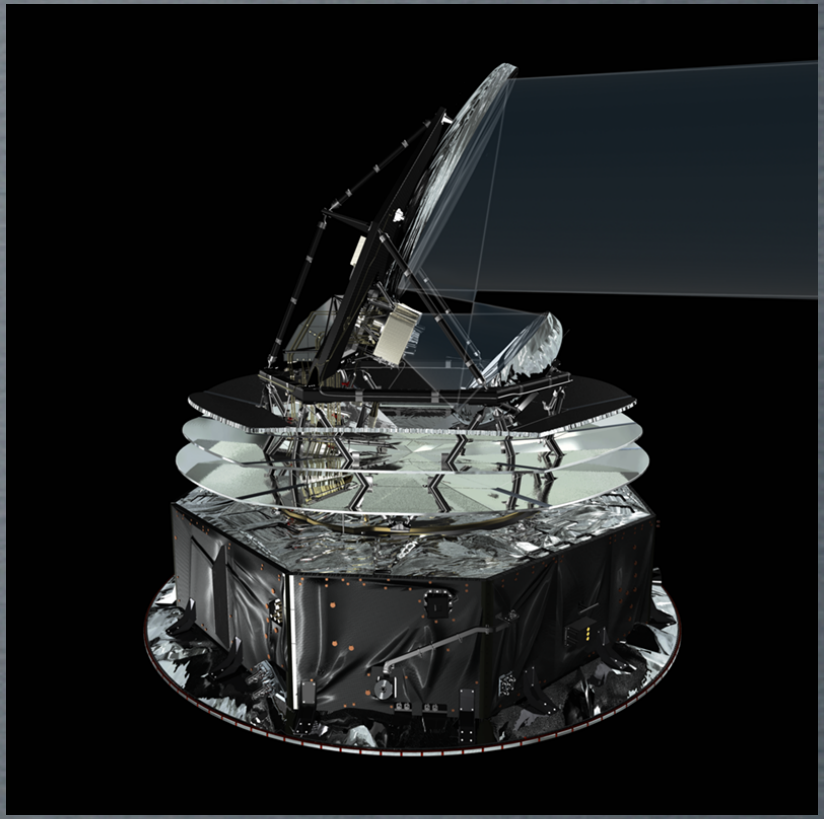

Instrument Characteristic	LFI			HFI					
Detector Technology	HEMT arrays			Bolometer arrays					
Center Frequency [GHz]	30	44	70	100	143	217	353	545	857
Bandwidth ($\Delta\nu/\nu$)	0.2	0.2	0.2	0.33	0.33	0.33	0.33	0.33	0.33
Angular Resolution (arcmin)	33	24	14	10	7.1	5.0	5.0	5.0	5.0
$\Delta T/T$ per pixel (Stokes I)^a	2.0	2.7	4.7	2.5	2.2	4.8	14.7	147	6700
$\Delta T/T$ per pixel (Stokes Q &U)^a	2.8	3.9	6.7	4.0	4.2	9.8	29.8	...	...

Planck bluebook, ESA-SCI(2005)1

Planck

- Comparison between COBE observations with WMAP (2 and 8 yr) and Planck (1 yr)

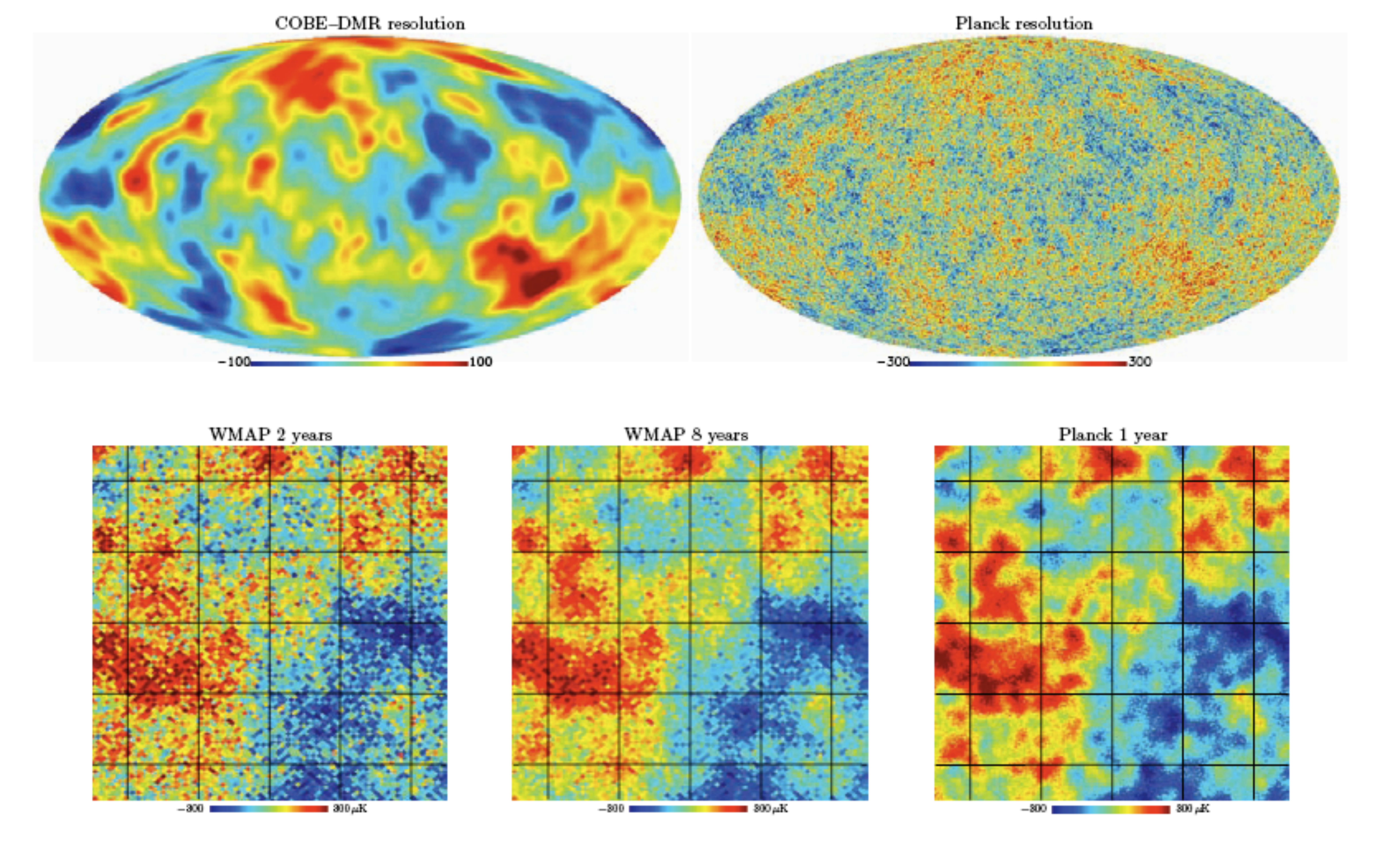

Planck bluebook, ESA-SCI(2005)1

Planck

- Forecasts for Planck
- Simulated power spectrum. WMAP-4yr and Planck 15 months simulated error bars

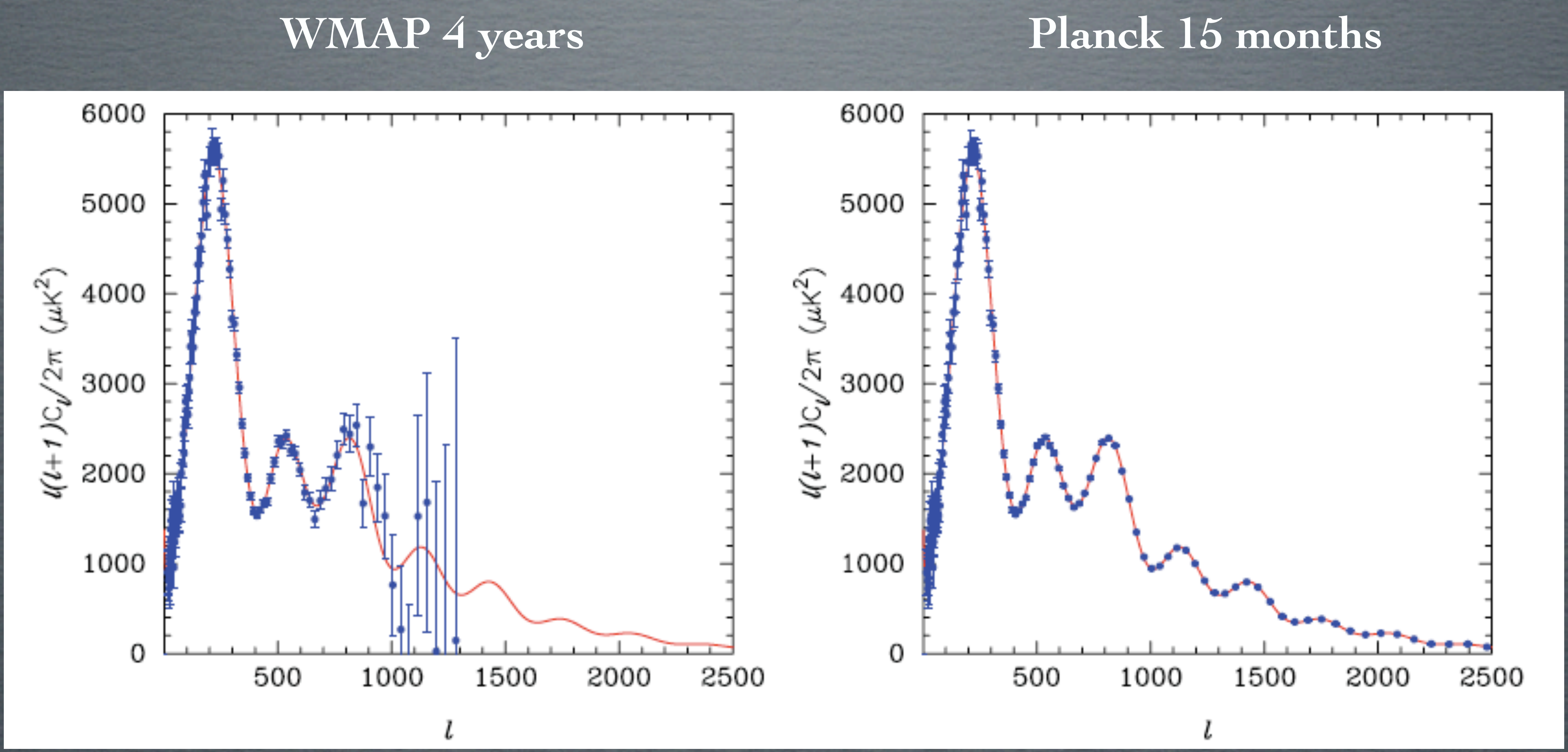

Planck bluebook, ESA-SCI(2005)1

The study of the polarization of the CMB

The importance of observing the CMB polarization

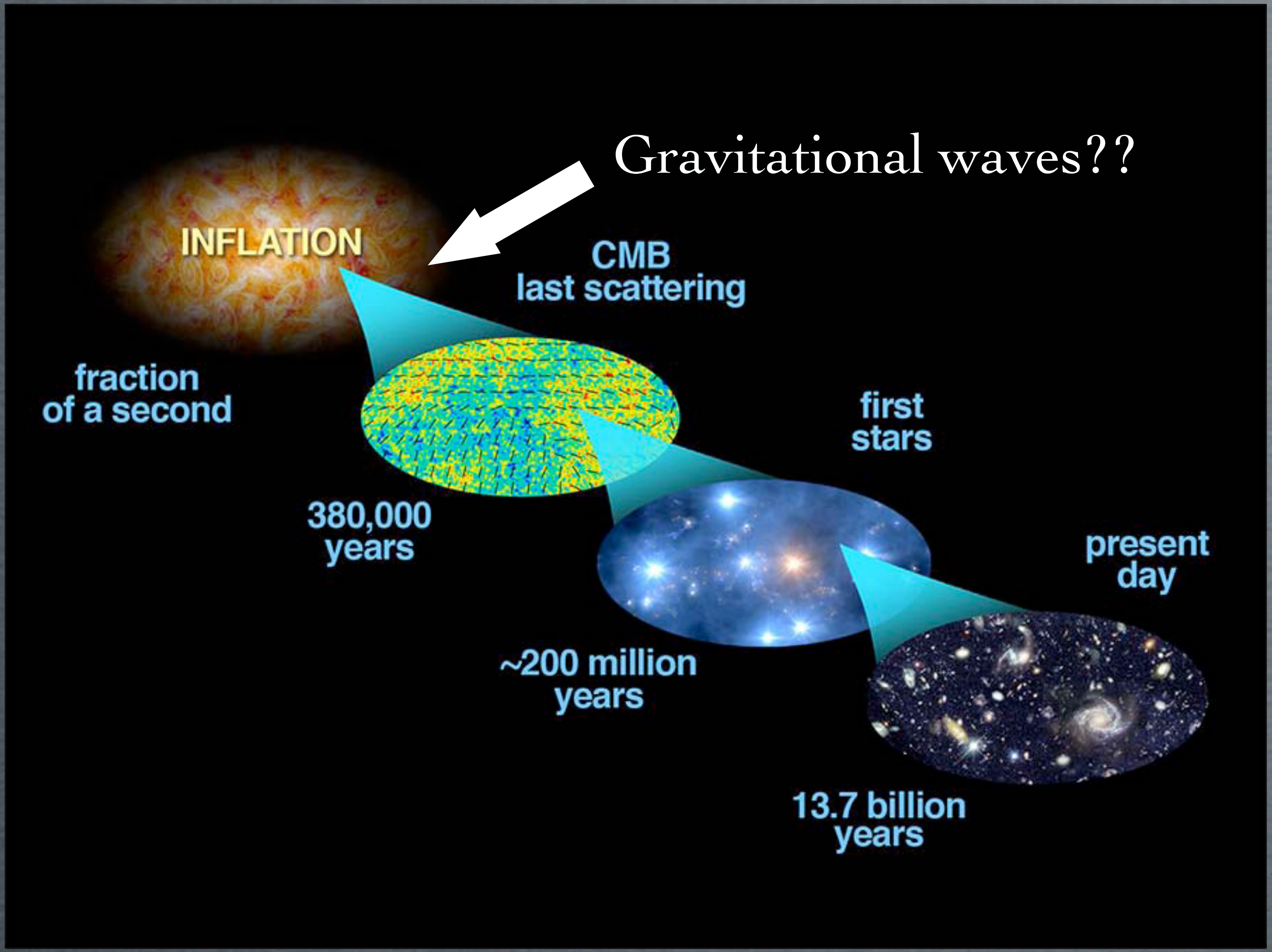

- Inflation is an epoch of very rapid expansion of the early Universe. Solves two mismatches of the ΛCDM model (horizon and flatness problems)
- Inflation is predicted to have generated a Gravitational Wave Background (GWB)
- This GWB should be observable as a B-mode anisotropy in the polarization pattern of the CMB

- Measuring or constraining that B-mode signal would provide important information about inflation and its energy scale. It would allow to select what inflation model agrees better with observations

The polarization of CMB anisotropies

❖ Fundamental prediction of the gravitational instability paradigm

❖ A net polarization is generated during recombination thanks to the quadrupole anisotropy in the radiation field

- For a multipole decomposition of the radiation field into spherical harmonics, the five quadrupole moments are represented by $l=2$, $m=0,\pm1,\pm2$
- Orthogonality of spherical harmonics $\Rightarrow$ only quadrupole moment can generate polarization from Thomson scattering
- The net polarization generated via Thomson scattering is linear $\Rightarrow$ the CMB will have non-zero Stokes parameters Q and U, and V=0

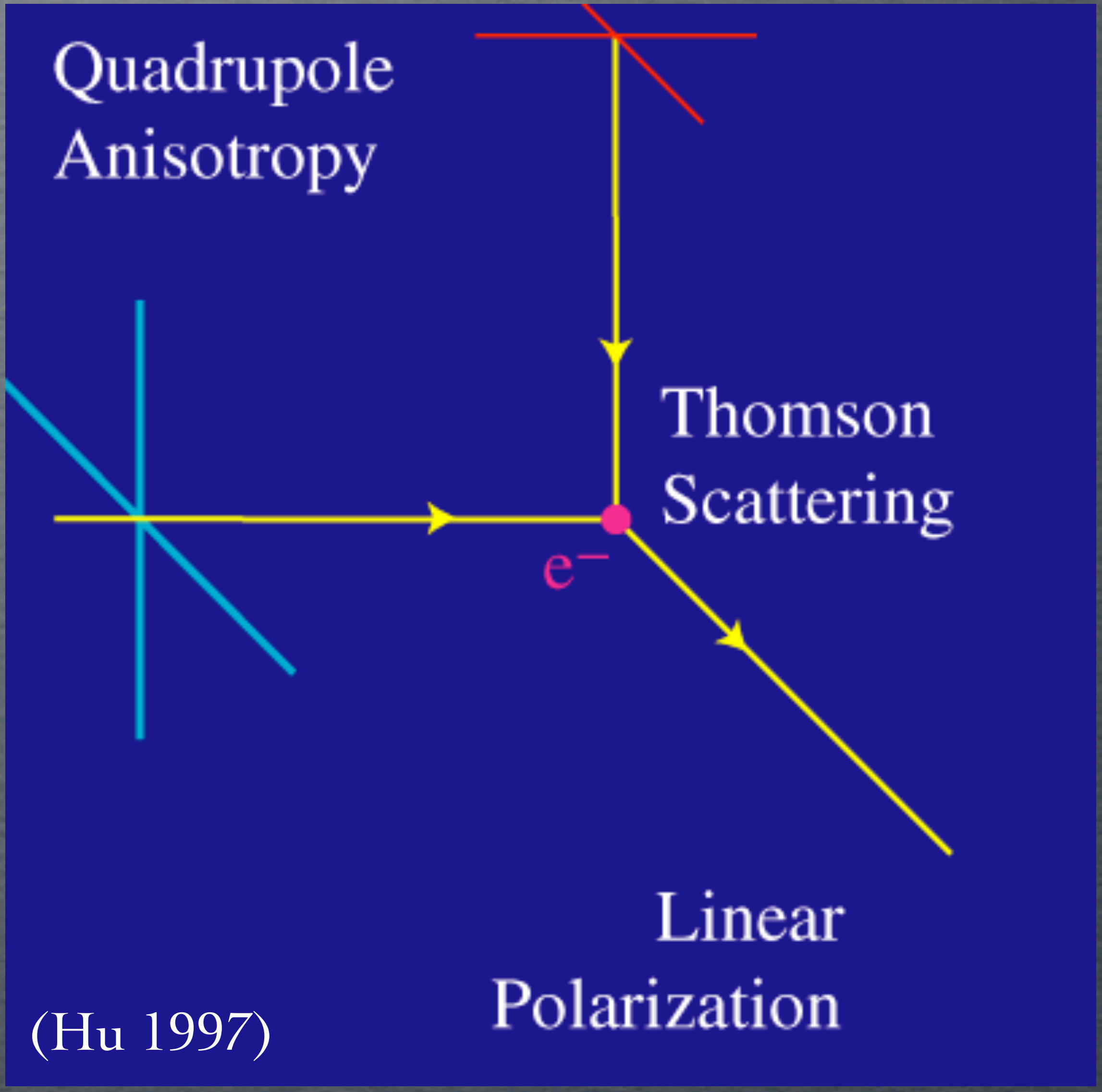

The polarization of CMB anisotropies

• Polarization maps can usually be decomposed into two different patterns, usually called E-modes (analog to gradient component) and B-modes (analog to curl component) - (Kamionkowski et al. 1997; Seljak & Zaldarriaga 1997)

• These two components are independent on the coordinate system and are related to the Q and U Stokes parameters by a non-local tranformation

• Physics of polarization generation. Different sources of anisotropies in the primordial Universe generate different types of modes

	E-modes	B-modes
Scalar (density perturbations)	Yes	No
Tensor (gravitational waves)	Yes	Yes

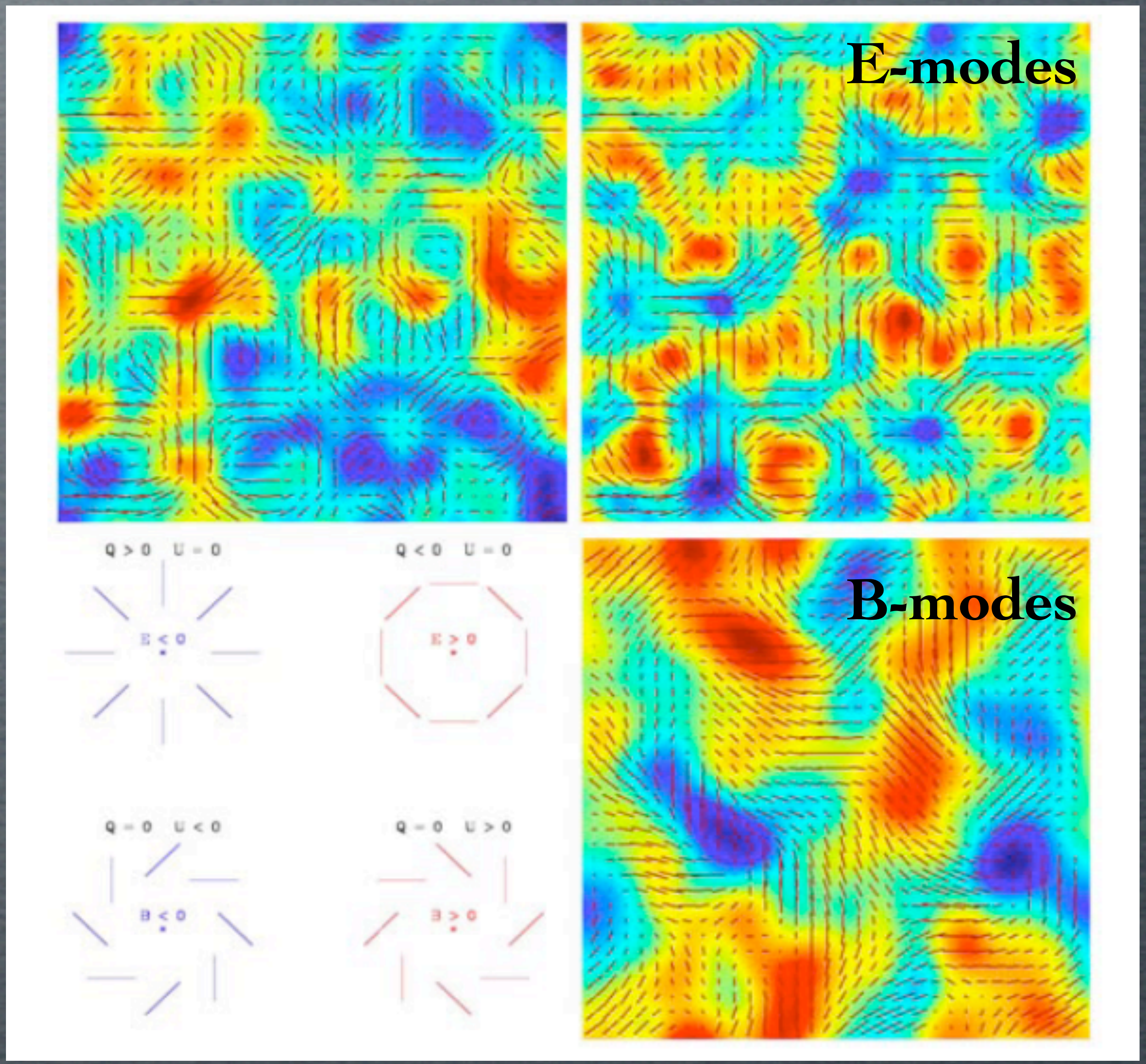

Primordial gravitational waves and B-modes

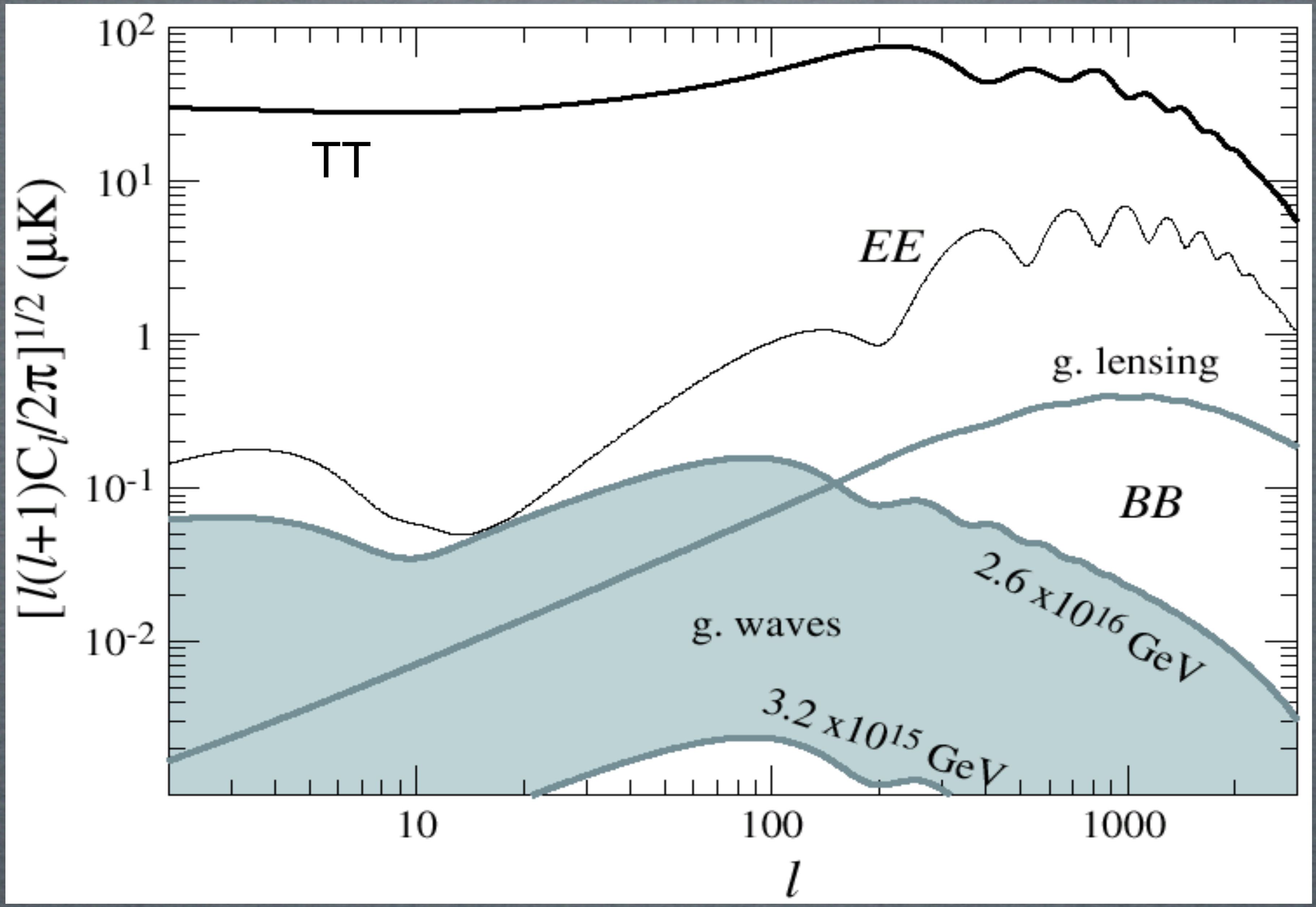

- r is the tensor to scalar ratio
- Proportional to the energy scale of inflation, which is proportional to the density of primordial gravitational waves

$$r = 0.001 \left(\frac{V}{10^{16}\ \mathrm{GeV}} \right)^4$$

- r=0.1 corresponds to a energy scale of inflation around the expected GUT value

Observability of B-modes

❖ Critical issues:

- Signals are extremely small ⇒ large number of receivers with large bandwidths are required
- Accurate control of systematics (cross-pol, spillover,...) is mandatory
- Foregrounds. B-mode signal is subdominant over Galactic foregrounds
  - Free-free, low-freq, not polarized
  - Synchrotron, low-freq, pol ~10%
  - Thermal dust, high-freq, pol ~10%
  - Anomalous emission, 20-60 GHz, pol ~3%?
  - Point sources, low-freq, pol ~5%

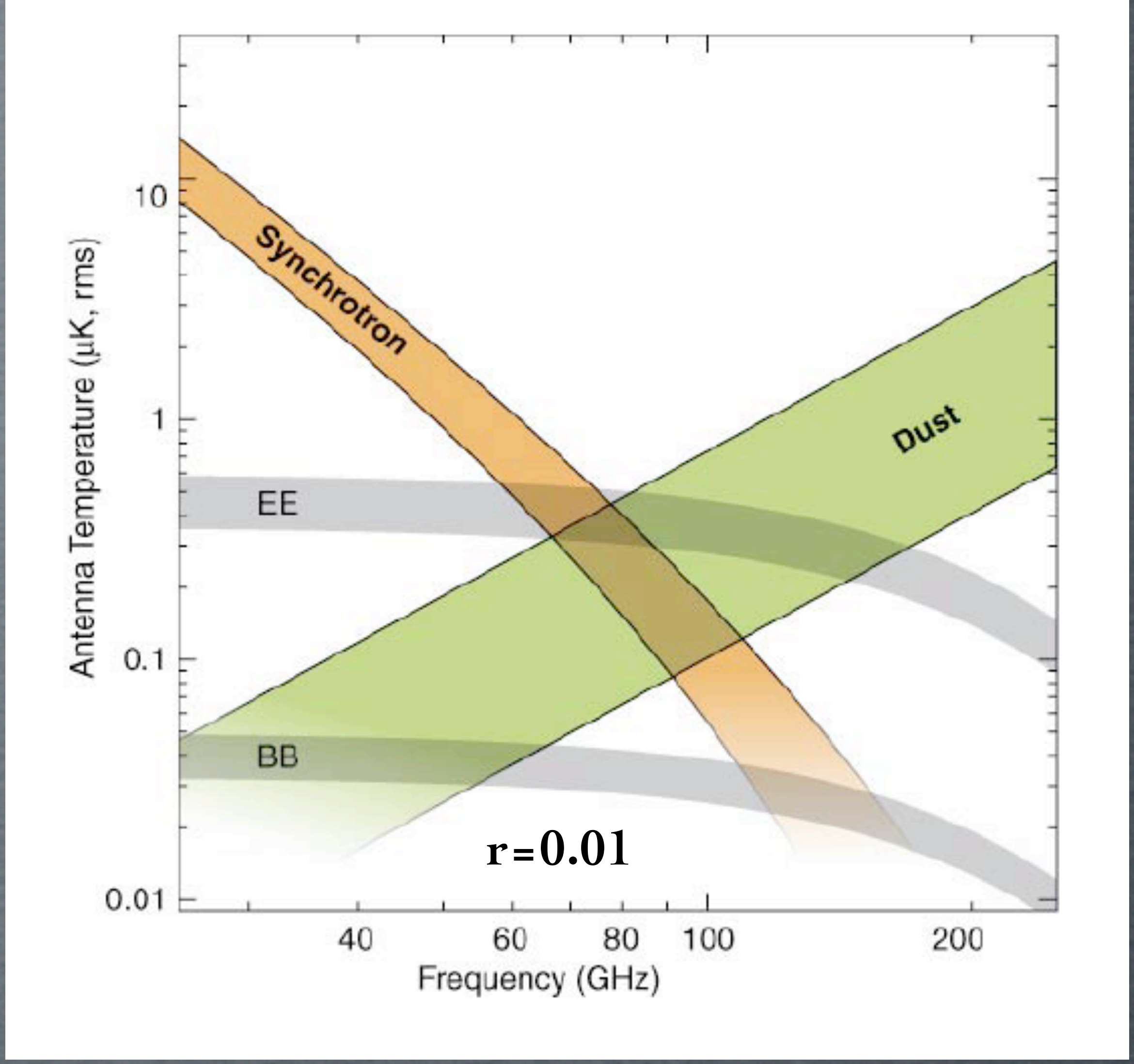

- Planck (launched May 2009; frequency range 30-800 GHz) will reach r~0.05
- Next generation missions: BPOL, planned for 2015-2020, will reach r~0.01-0.001
- Systematic program to study polarized astrophysical foreground signals is needed (see NASA-NSF report "Task Force on CMB research" and ESA-ESO report on "Fundamental cosmology")

Polarization experiments

❖ Ground-based: DASI, Polatron, ACT, CBI, KuPID, AMiBA, SPTPol, QUAD, CAPMAP, BICEP, QUIET, PolarBear, ClOVER, BRAIN, QUIJOTE

❖ Balloon: Archeops, BOOMERanG, MAXIPOL, EBEX, SPIDER

❖ Space: WMAP, PLANCK, BPOL

EBEX

(Grainger et al 2008)

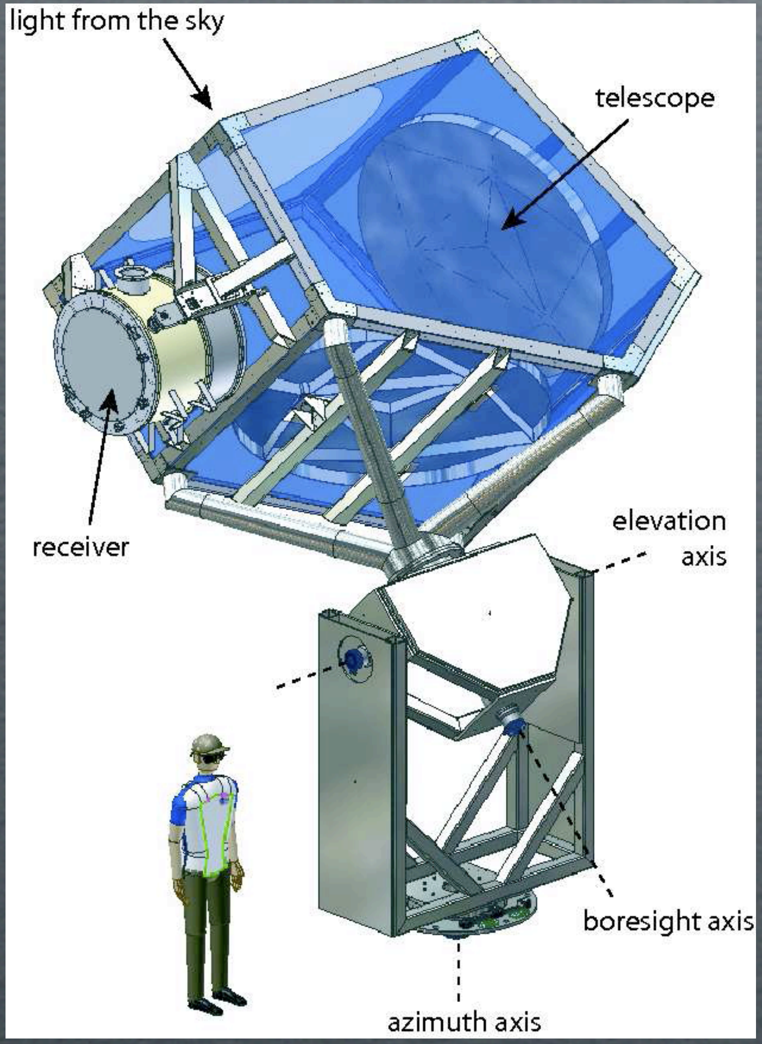

ClOVER

(North et al 2008)

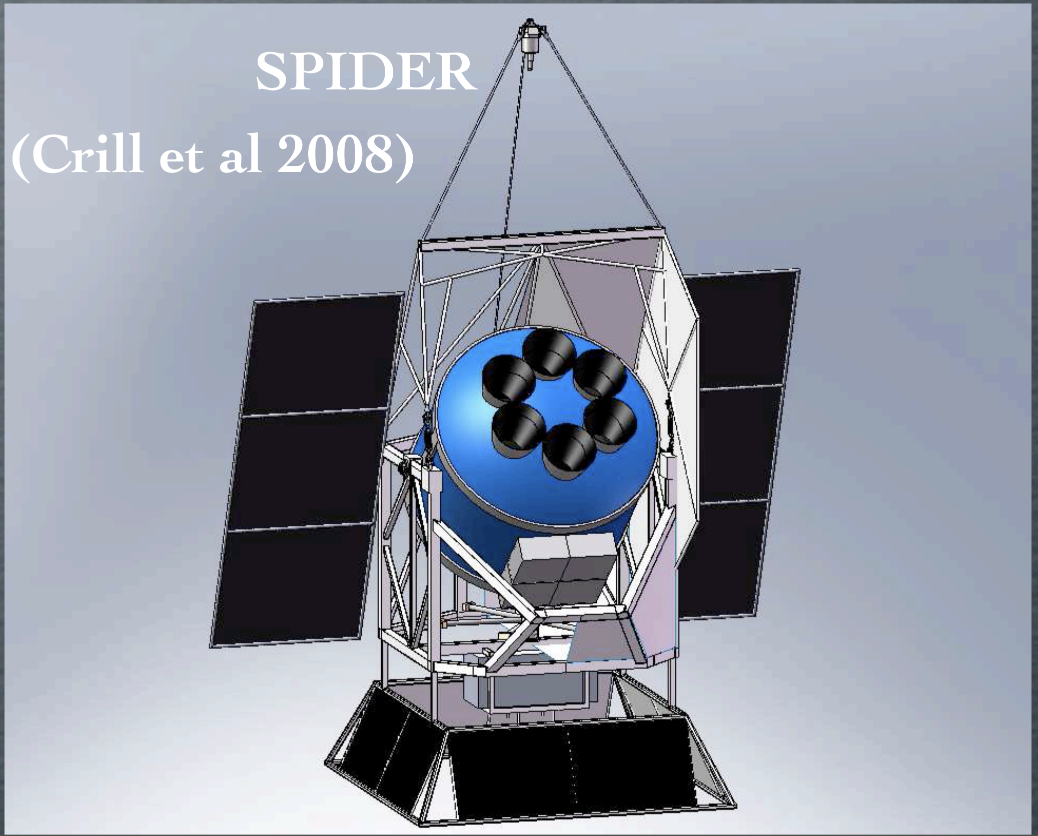

SPIDER

(Crill et al 2008)

Current observational status

❖ E-mode signal: detected by DASI (Kovac et al. 2002, Nature), CBI, CAPMAP, Boomerang, WMAP, QUAD

❖ B-mode signal: current upper limits are $r<0.73$ (95% CL; Chiang et al. 2009) from BICEP, $r<0.4$ (95% CL; Hinshaw et al. 2009) from WMAP5, or $r<0.22$ (95% CL, Komatsu et al. 2009) combining WMAP5 with SN Ia and SDSS

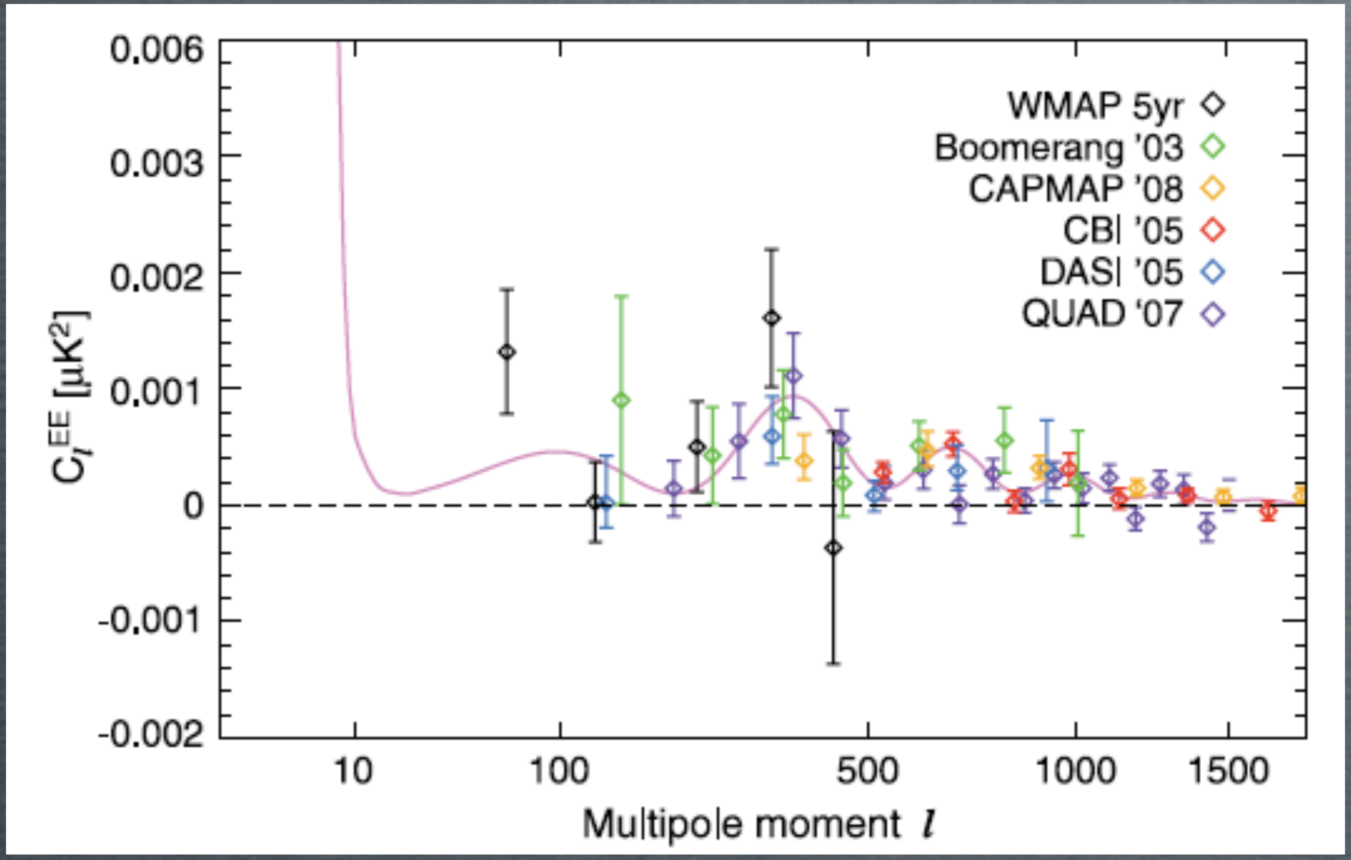

Current observational status of the E-modes (Nolta et al. 2009)

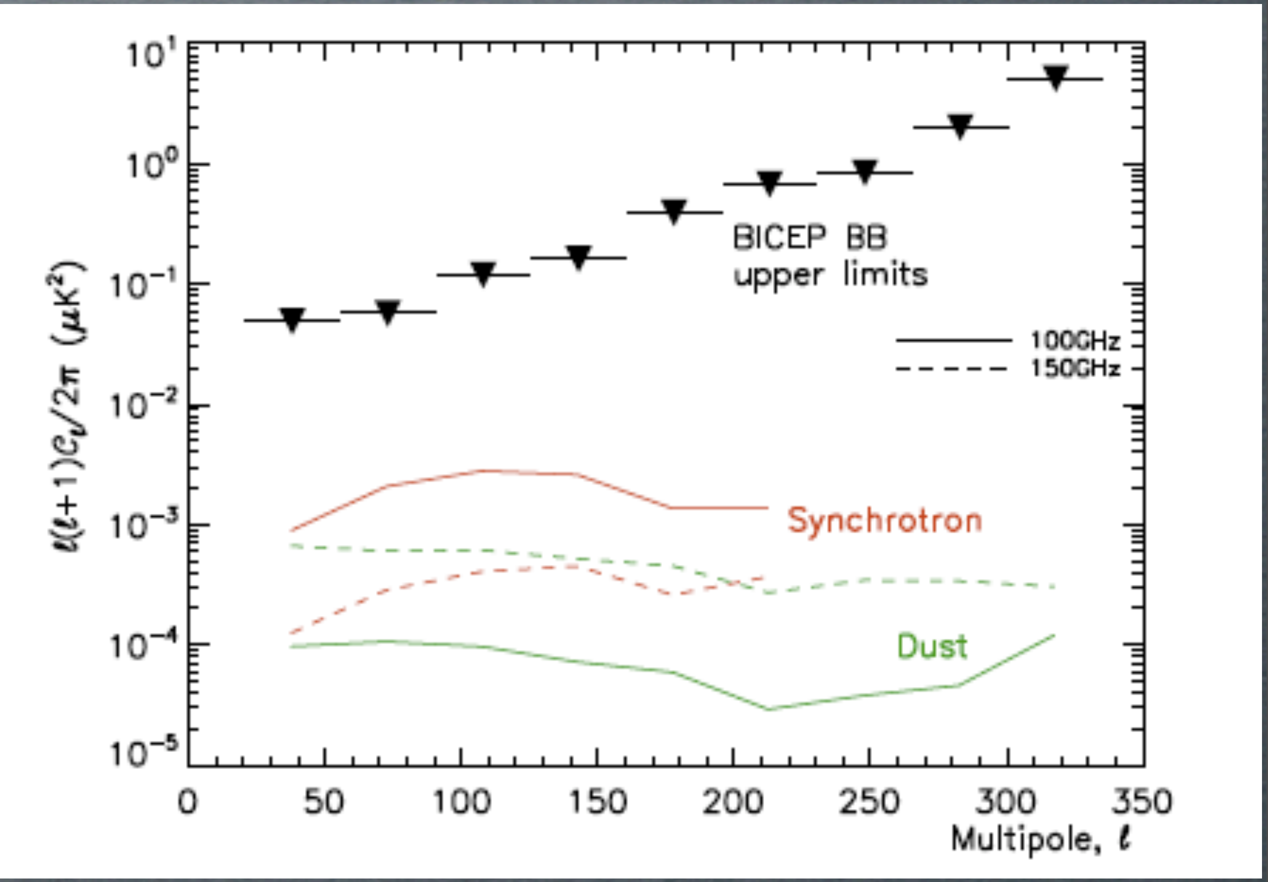

B-mode signal upper limits from BICEP data (Chiang et al. 2009)

The QUIJOTE-CMB experiment

The QUIJOTE CMB collaboration

- **Instituto de Astrofísica de Canarias (IAC)**

  R. Rebolo (PI), J.A. Rubiño-Martín (PS), R. Génova-Santos, F. Gómez-Reñasco, J.M. Herreros (PM), S. Hildebrandt, R. Hoyland (InstS), C.H. López-Caraballo, M.Tucci

- **Instituto de Física de Cantabria**

  E. Martínez-González, B. Barreiro, F.J. Casas, R. Fernández-Cobos, D. Herranz, M. López-Caniego, P. Vielva

- **DICOM - Universidad de Cantabria**

  E. Artal, B. Aja, J.L. Cano, L. de la Fuente, A. Mediavilla, J.P. Pascual, E. Villa

- **JBO - University of Manchester**

  L. Piccirillo, R. Battye, R.D. Davies, R.J. Davis, C. Dickinson, B. Maffei, G. Pisano, R.A. Watson

- **University of Cambridge**

  K. Grainge, M.P. Hobson, M. Brown, A. Challinor, A.N. Lasenby, R.D.E. Saunders, P.F. Scott, H. Smith

- **IDOM**

  J. Ariño, B. Etxeita, A. Gómez, C. Gómez, G. Murga, J. Pan, R. Sanquirce, A. Vizcargüenaga

The Q-U-I JOint TEnerife CMB experiment

❖ **Goal:** to perform high sensitivity observations of the polarization of the CMB and Galactic foregrounds at low frequencies (11-40 GHz) and large angular resolution (1º)

❖ **Main science driver:**

- To constrain (or to detect) primordial B-modes down to $r=0.05$
- To measure and characterize foregrounds (synchrotron, anomalous emission) with unprecedented sensitivity at 10-20 GHz, allowing correction in future space missions aiming at $r\sim0.001$

The Q-U-I JOint TEnerife CMB experiment

❖ **Project baseline:**

- **Site:** Teide Observatory (altitude: 2400 m), Spain
- **Angular resolution:** 1 degree
- **Telescope and instruments:**

  - Phase I: First Telescope, equipped with the First Multifrequency Instrument with channels @ 11, 13, 17, 19 and 30 GHz (funded, starts operation Feb. 2010). Second Instrument with 16 polarimeters @ 30 GHz (funded, starts operation by Apr. 2011). Polarized Source Subtractor (built, starts operation Feb. 2010)
  - Phase II: Second Telescope, with a Third Instrument @ 40 GHz (or 90 GHz)
  - Phase III: new concepts. Replicate at southern hemisphere?

❖ **Polarization detection:** modulation (similar to half-wave plate)

❖ **Observing strategy:** each antenna mounted on a fast-spinning system (0.1-0.25 Hz), performing scans on azimuth at a constant elevation. Earth rotation provides a daily sky coverage of several thousands square degrees.

❖ **Sensitivity and sky coverage for Phase I:**

- Sensitivity of ~ 3-4 μK/beam after 1 year over 3,000-10,000 deg^2 with the First Instrument (11-19 GHz), and of ~0.5 μK/beam after 3 years with the Second Instrument (30 GHz)
- This will permit to reach r=0.1 by 2013 and r=0.05 by 2016

QUIJOTE site: the Teide Observatory

❖ The Teide Observatory is run by the IAC

❖ Altitude: 2400 m a.s.l.

❖ Geographical coordinates: 16º 30’ W and 28º 18’ N

❖ Temperature inversion layer 1200-1500 m. Very dry and stable atmosphere above

❖ Previous experience with other CMB experiments indicates 90% of the time data is system noise limited

❖ Typical PWV ~2-4 mm and RH ~15-25%

❖ Transmissivity ~90% ⇒ $T_{sky} \sim 5$ K

❖ Easy road access: 40 km road journey from IAC

(http://www.iac.es/eno.php?op1=3&lang=en)

QUIJOTE site: the Teide Observatory

(Image from Google maps)

QUIJOTE basic design

Phase I

- Funded
- First telescope
- First Instrument (10-30 GHz)
- Second Instrument (30 GHz)
- Installed in 2009

Phase II

- Not funded
- Second telescope
- Third Instrument (40 GHz)
- Starts in 2010/2011

QUIJOTE platform and enclosure

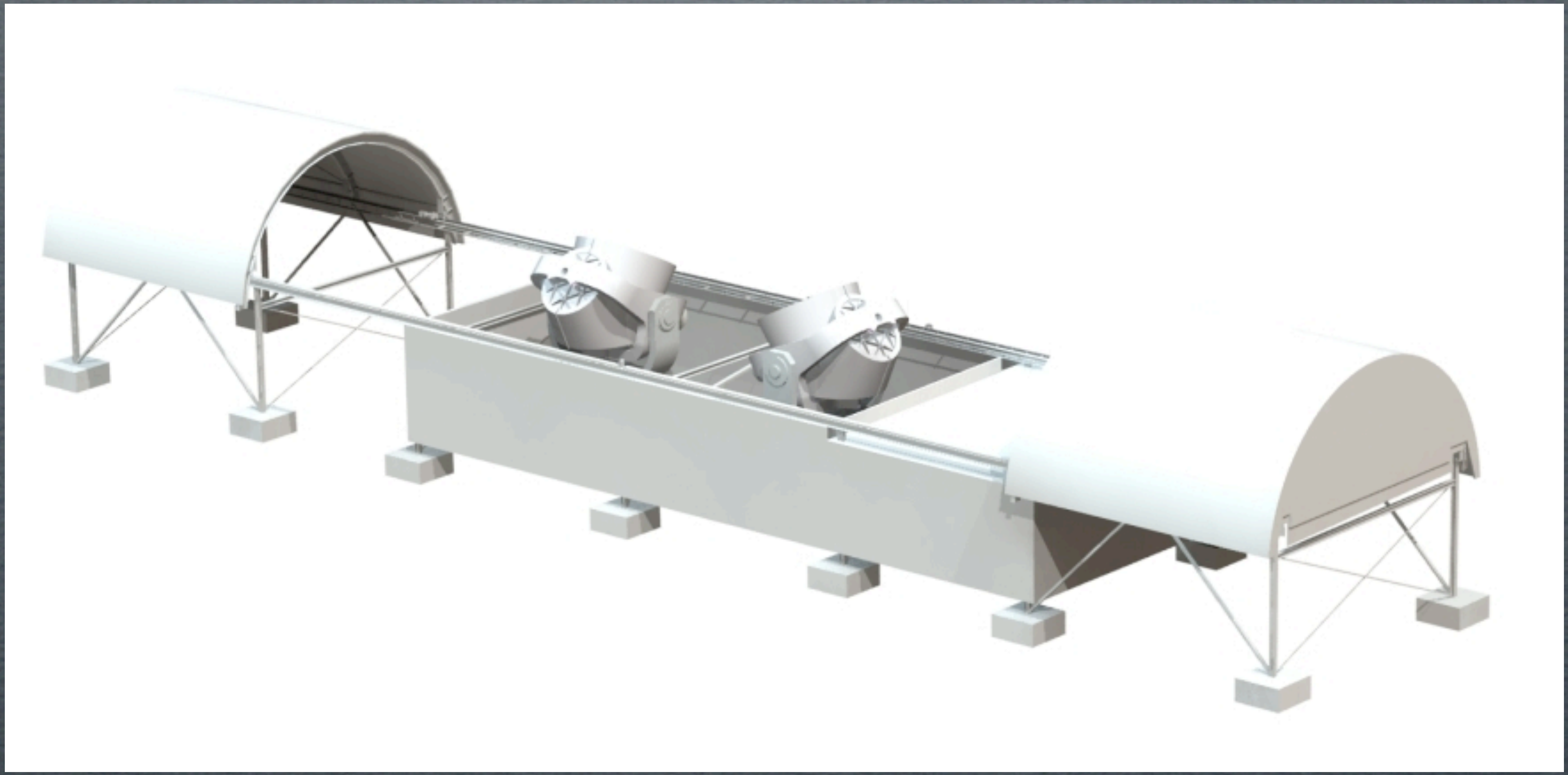

QUIJOTE First Telescope design

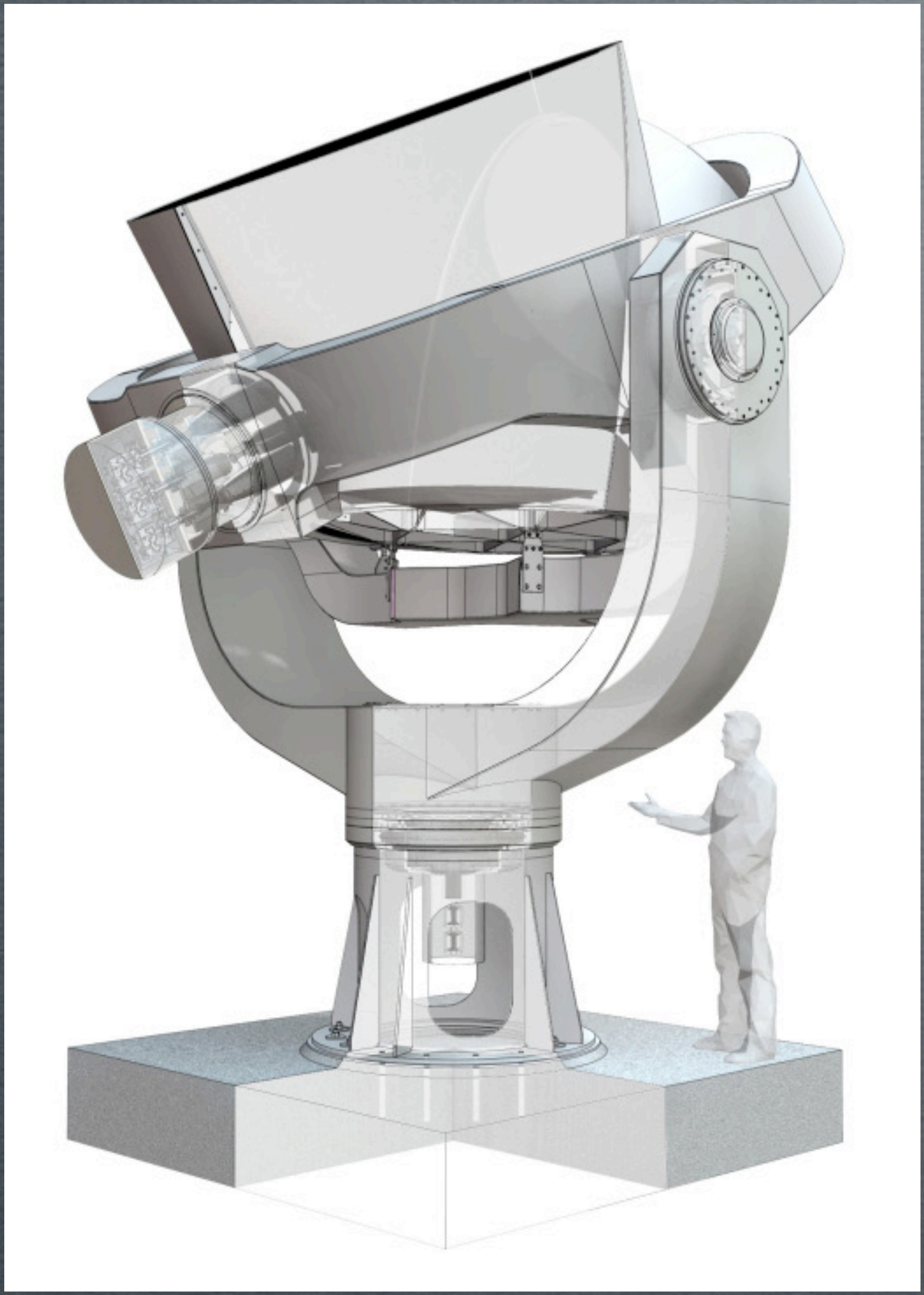

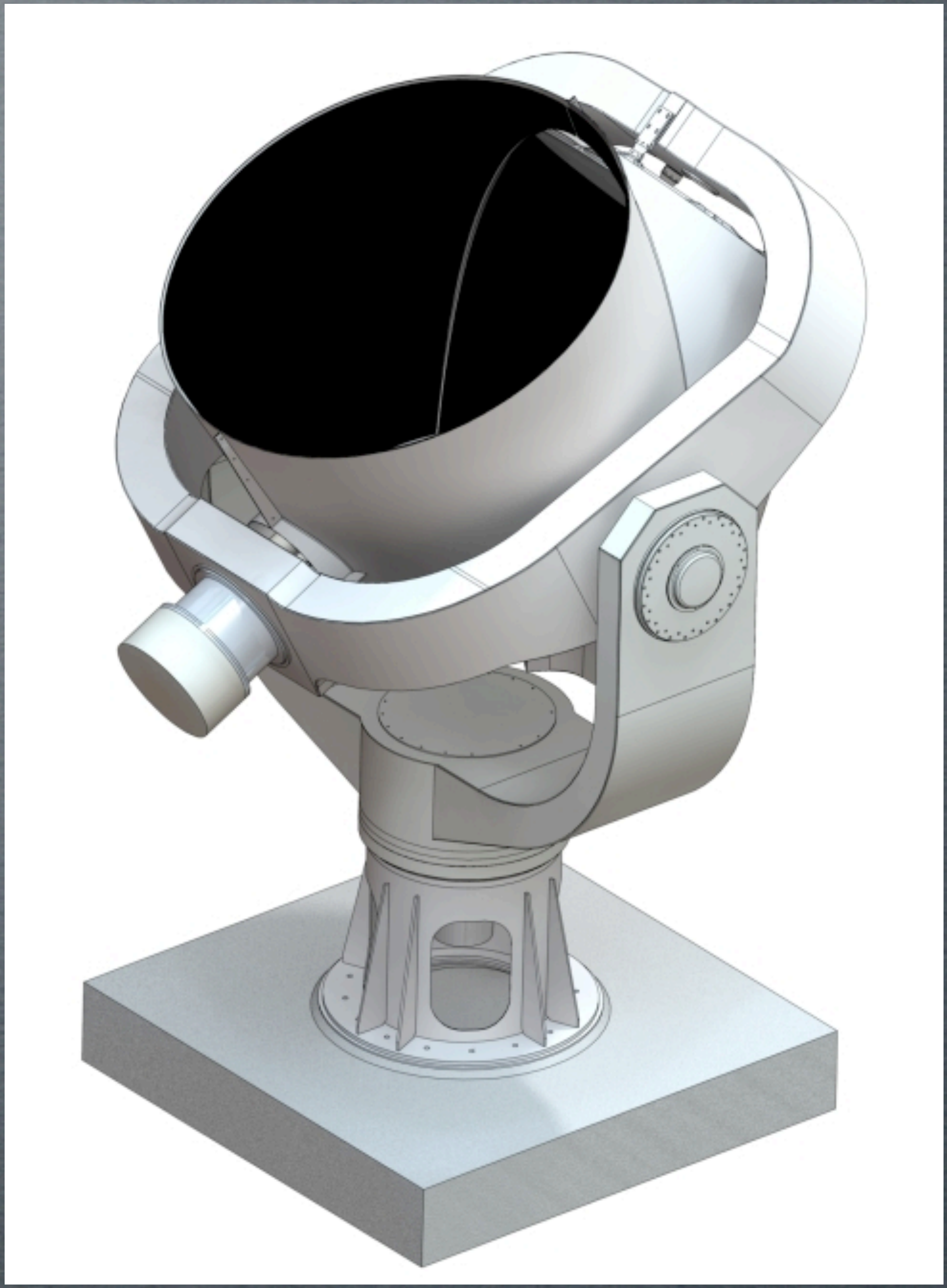

QUIJOTE telescope. Mount and optics

- Alto-azimutal mount
- Maximum rotation speed around AZ axis: 0.25 Hz
- Maximum zenith angle: 60º
- Cross-Dragonian design
- Aperture: 3 m (primary) and 2.6 m (secondary)
- Maximum frequency: 90 GHz (rms≤20μm and max deviation =100 μm)

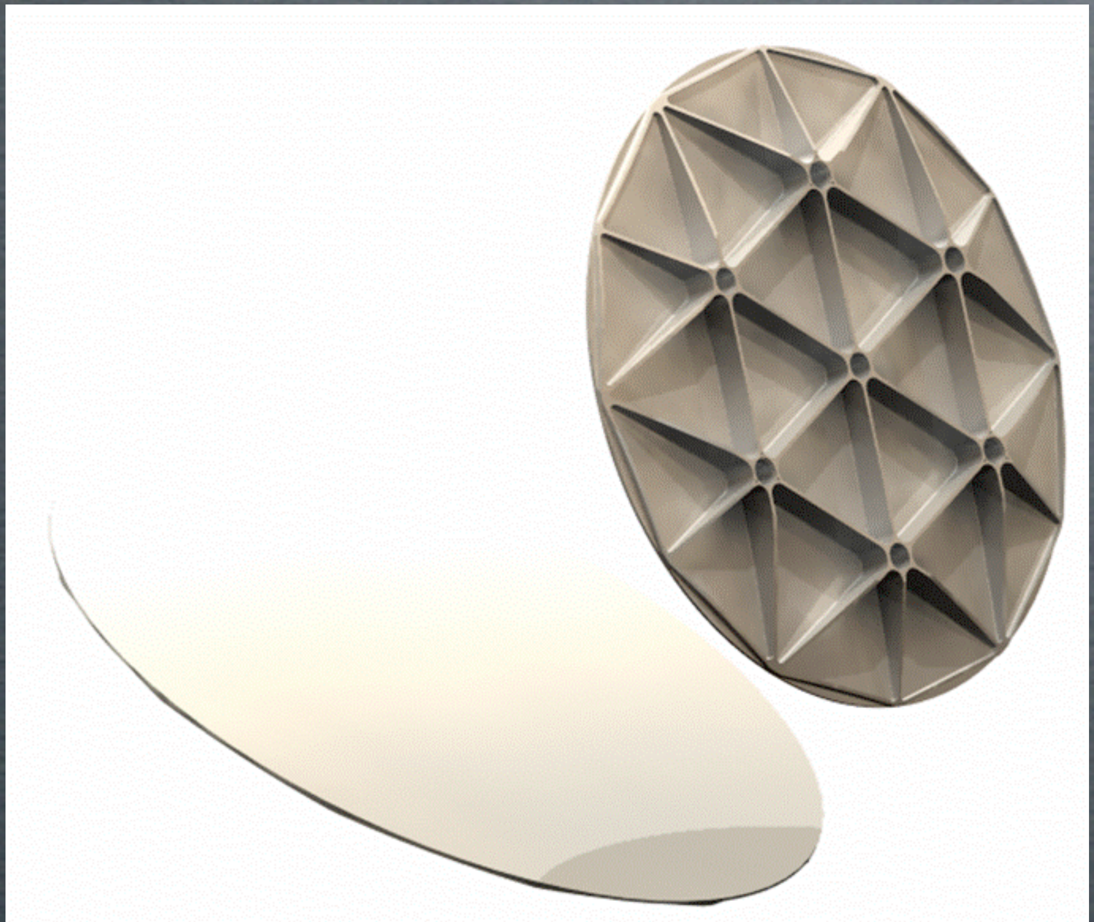

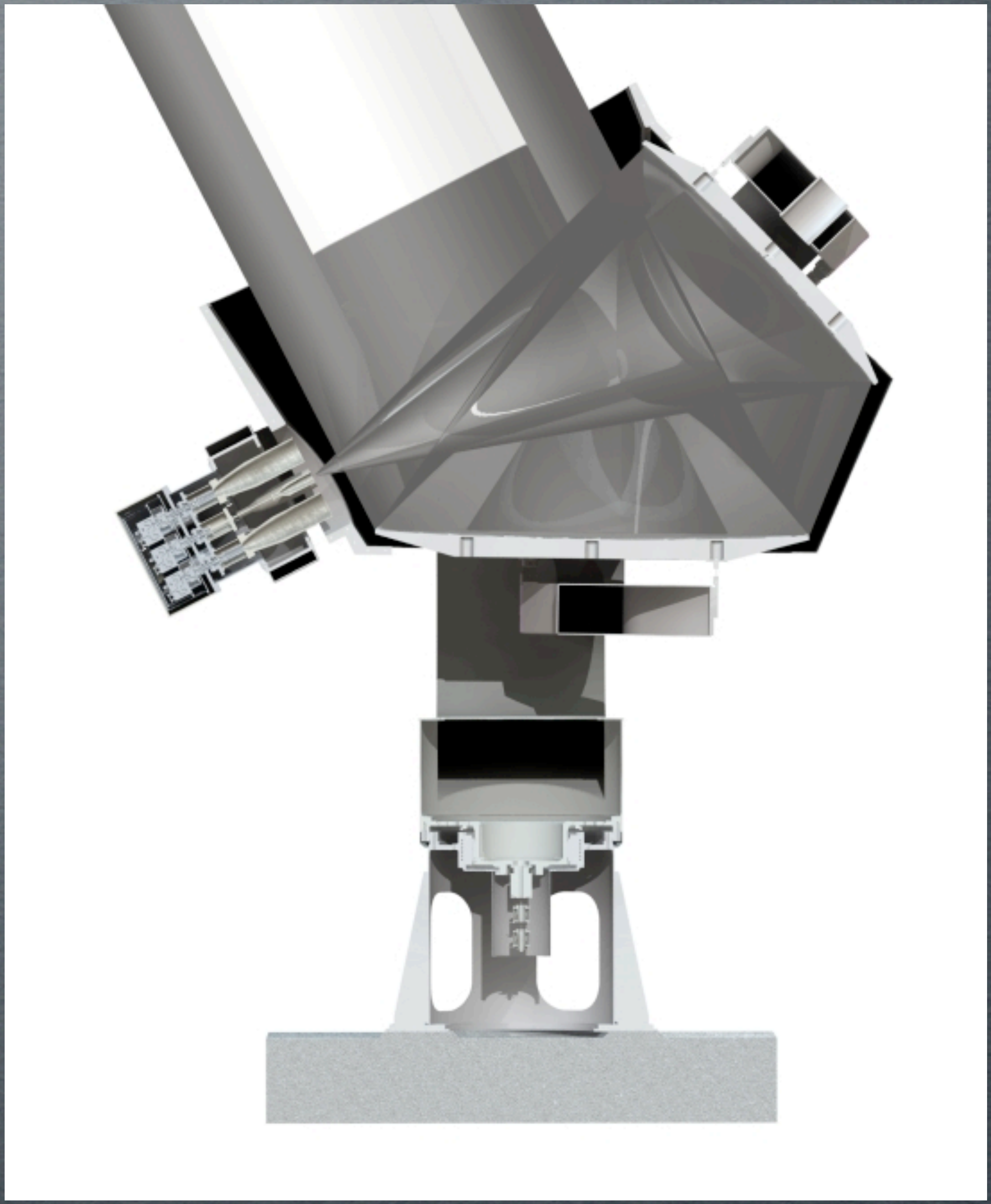

QUIJOTE First Telescope

- Assembly at IDOM

- Shipment:

QUIJOTE First Telescope

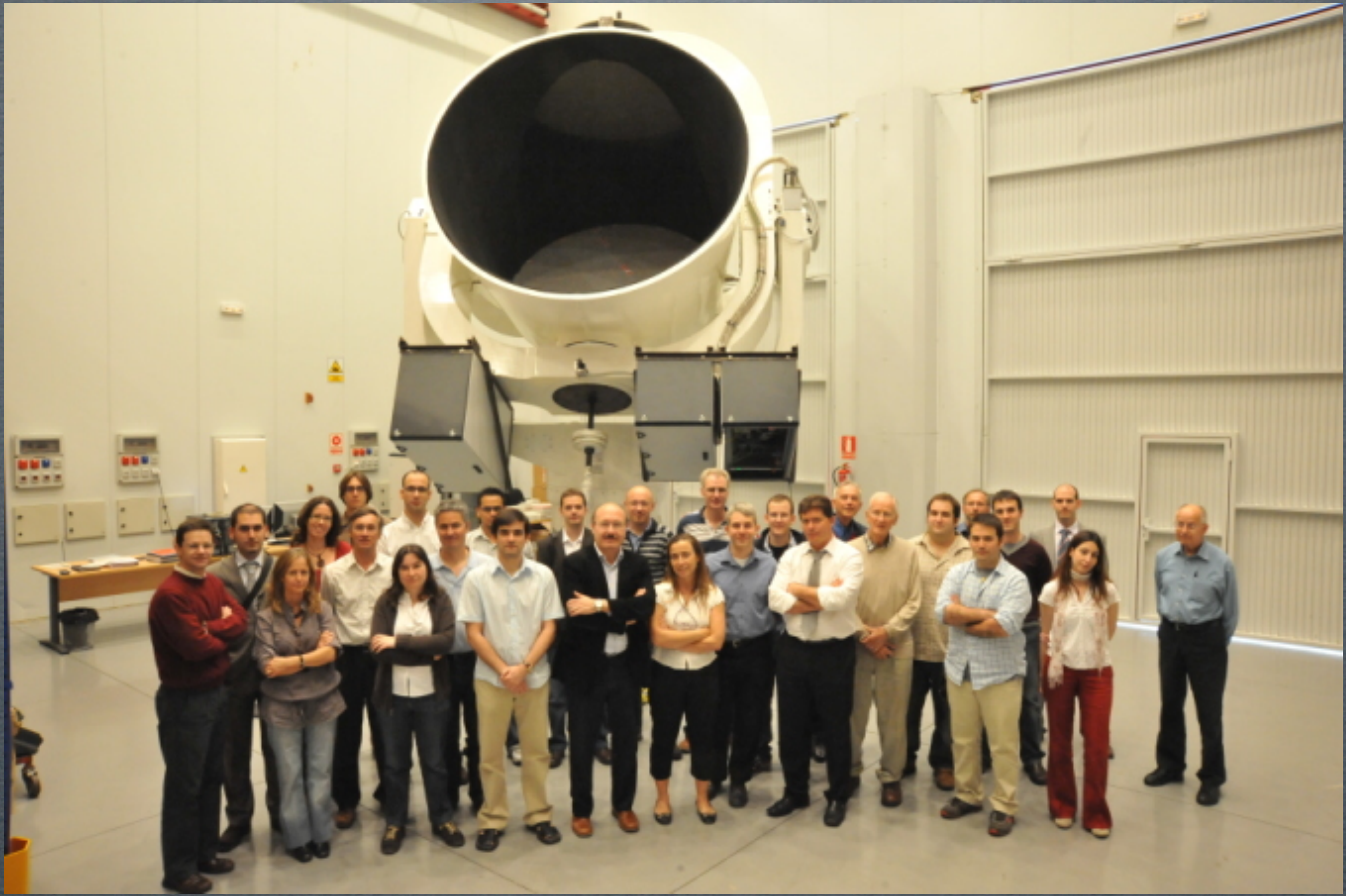

QUIJOTE First Instrument

- 5 conical corrugated feedhorns (B. Maffei at JBO), with optimal cross-polarization properties (≤ -35dB) and providing symmetric beams
- Polar modulator spinning at speeds up to 40 Hz (polar modulation 160 Hz)
- Wide-band cryogenic Ortho-Mode-Transducer (OMT)
- MMIC 6-20 GHz Low Noise Amplifiers (LNAs; S. Weinreb, Caltech). Gain: 30dB. T_{noise}=9K. Faraday module for the 30 GHz FEM (same as for OCRA-f)
- BEM built by DICOM and IFCA
- Cryogenics and mechanical system by CMS and IDOM

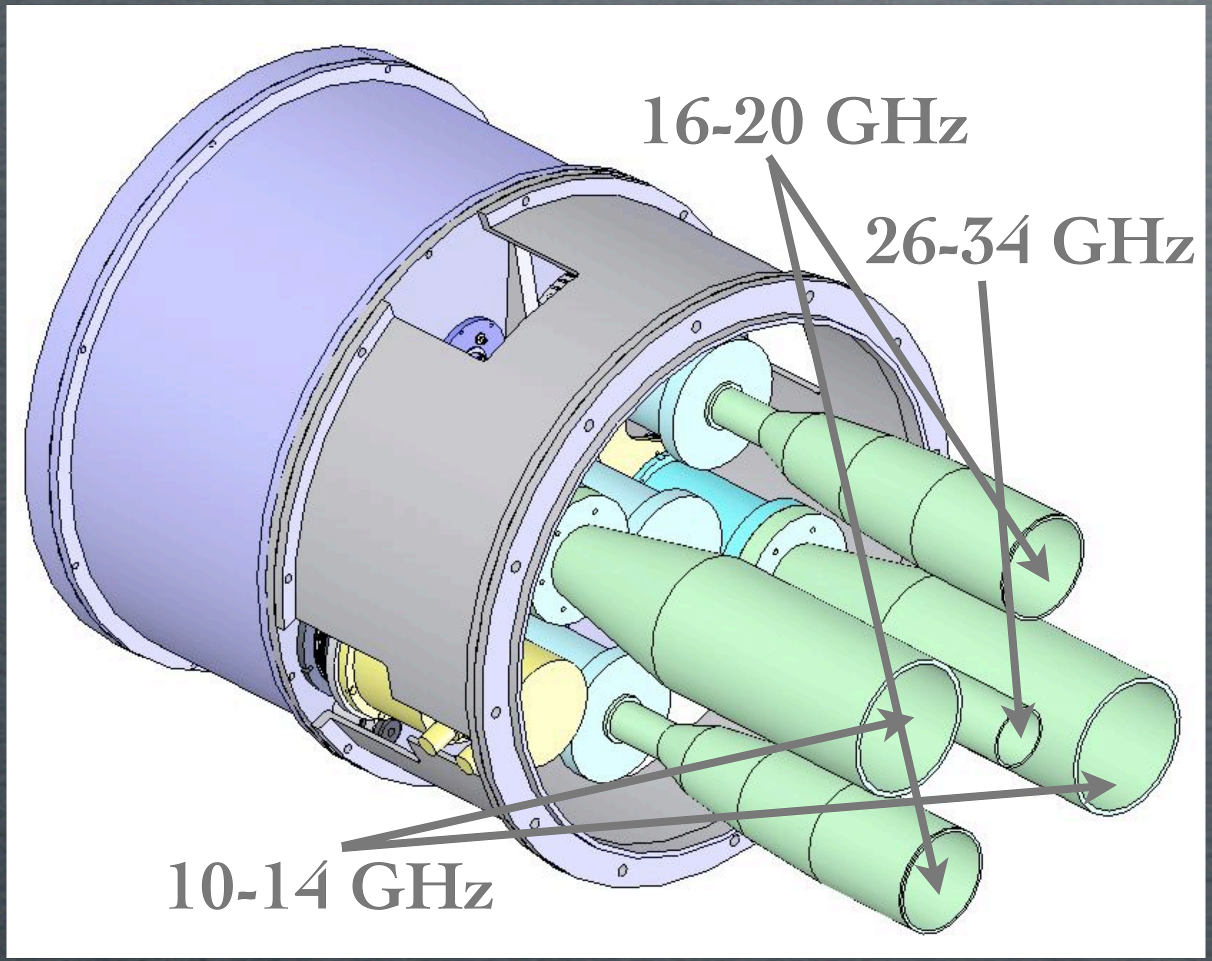

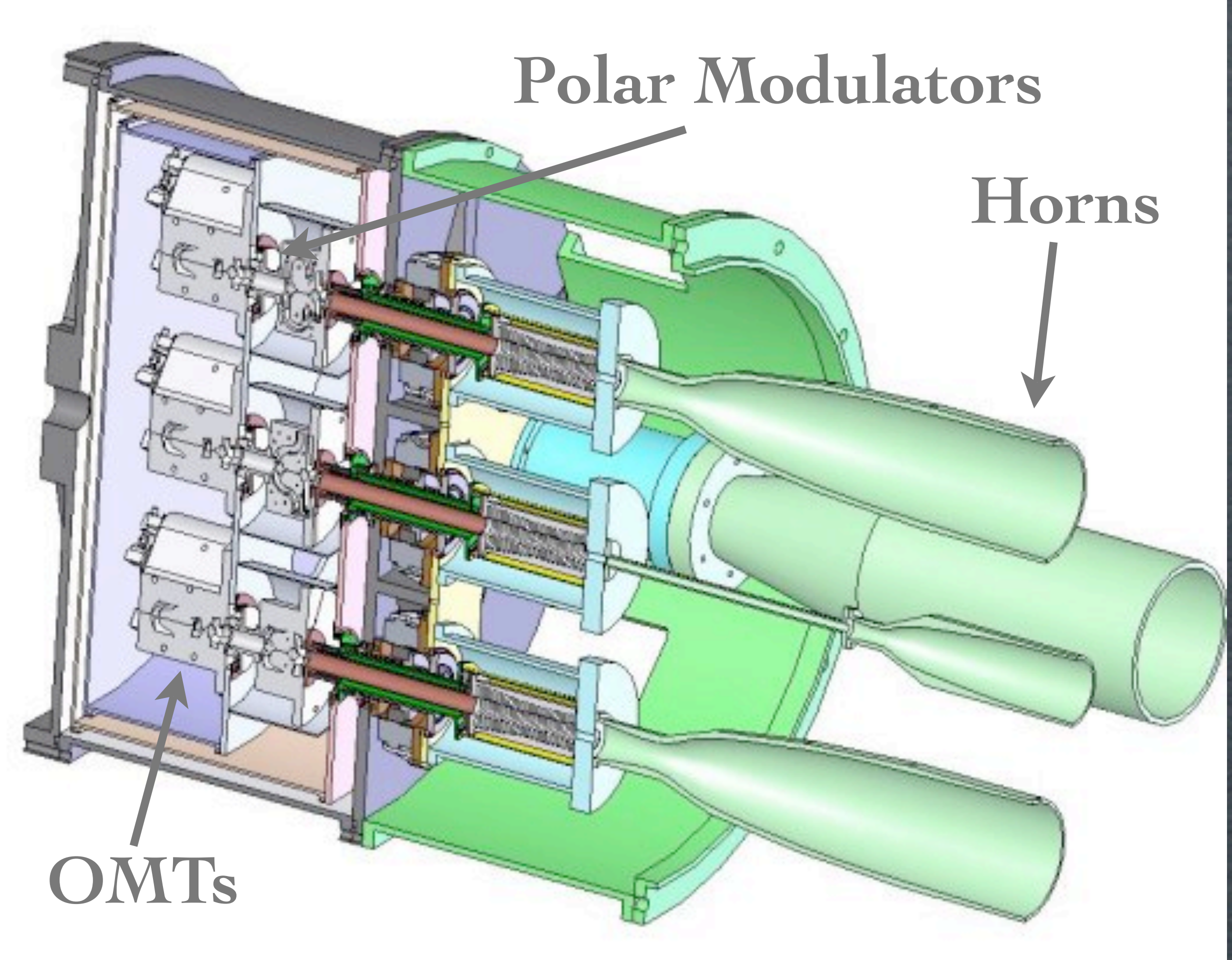

QUIJOTE First Instrument

OMTs (UC/IAC)

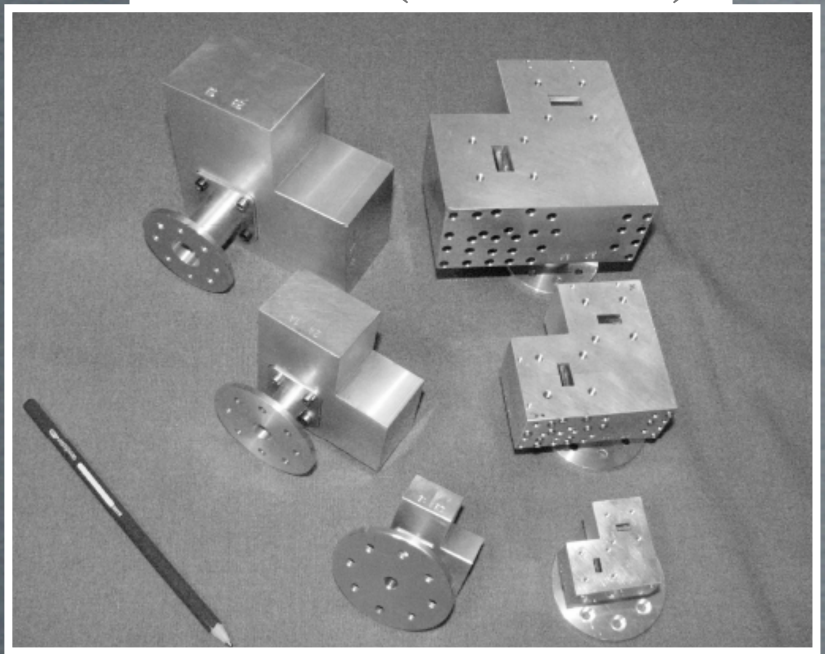

PMs (UC/IAC)

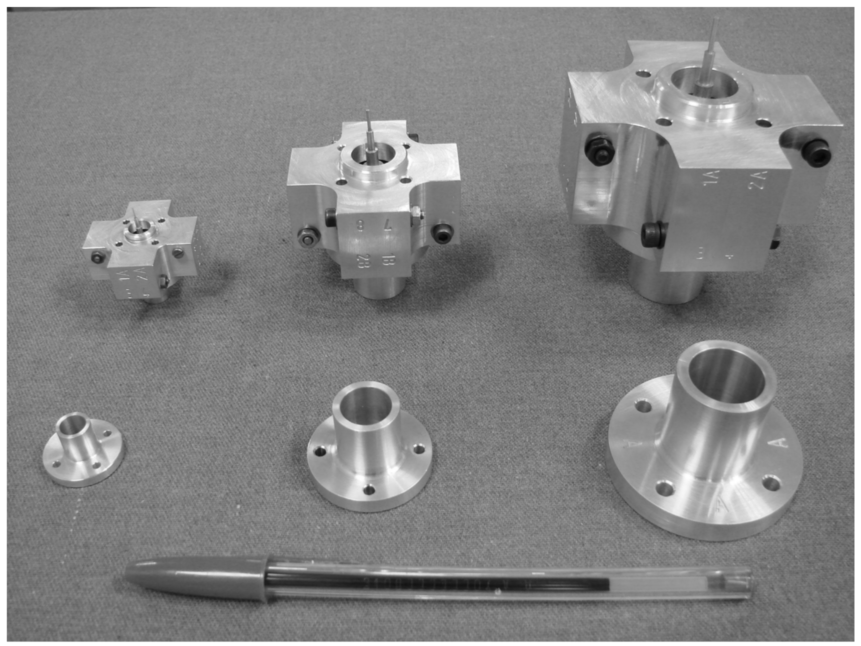

Internal feedhorns

QUIJOTE First Instrument. Receiving system

First instrument cryostat

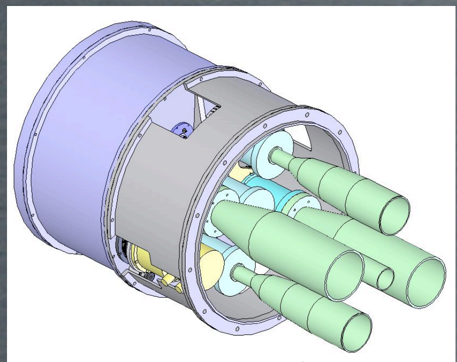

OMT

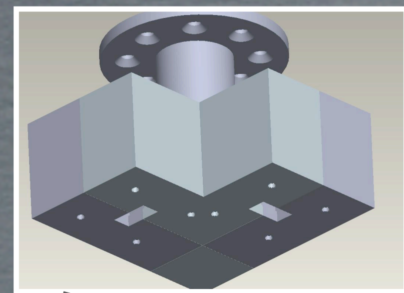

LNA 6-20 GHz

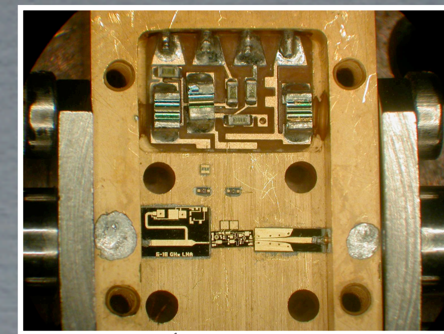

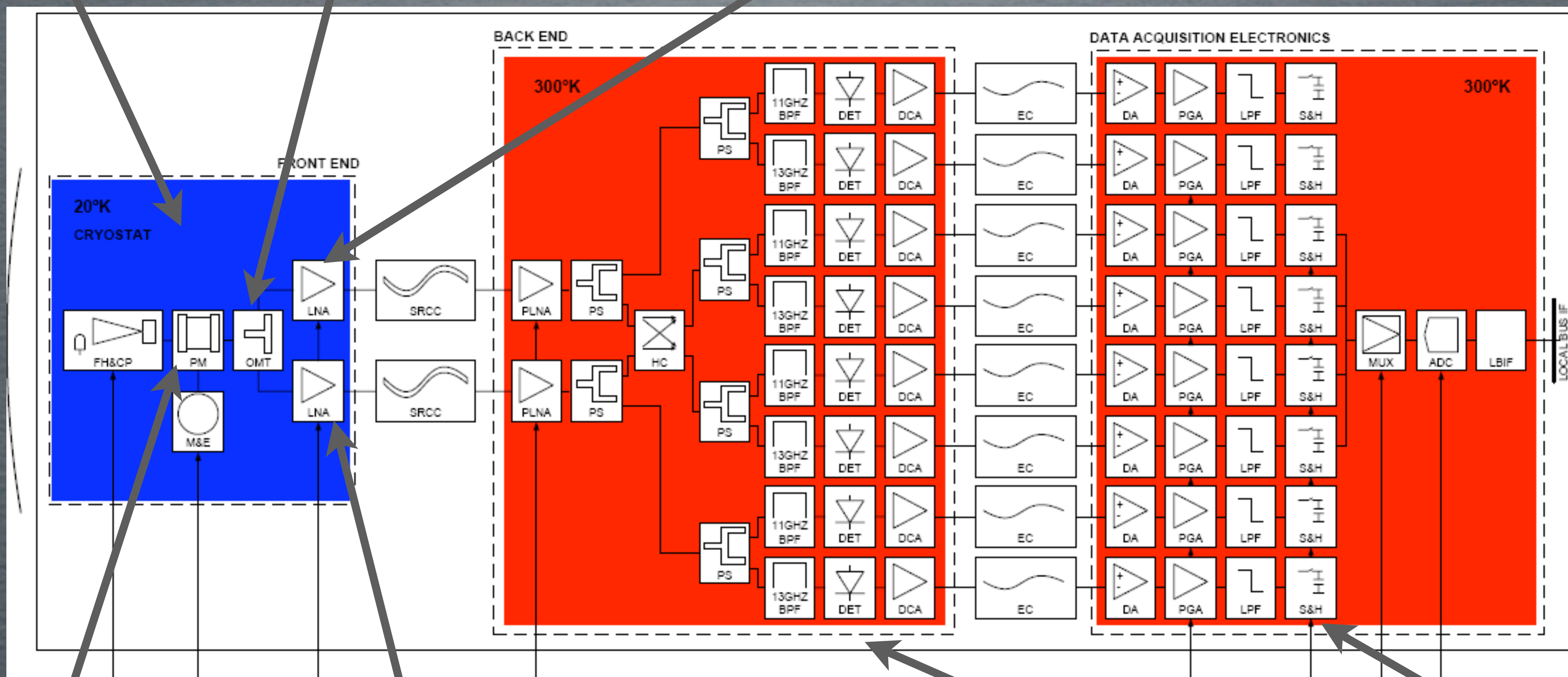

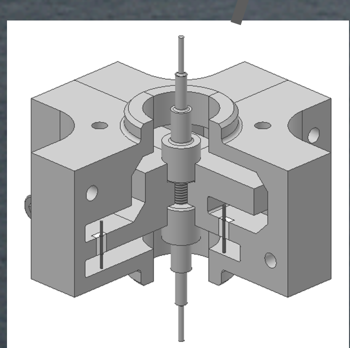

Polar modulator

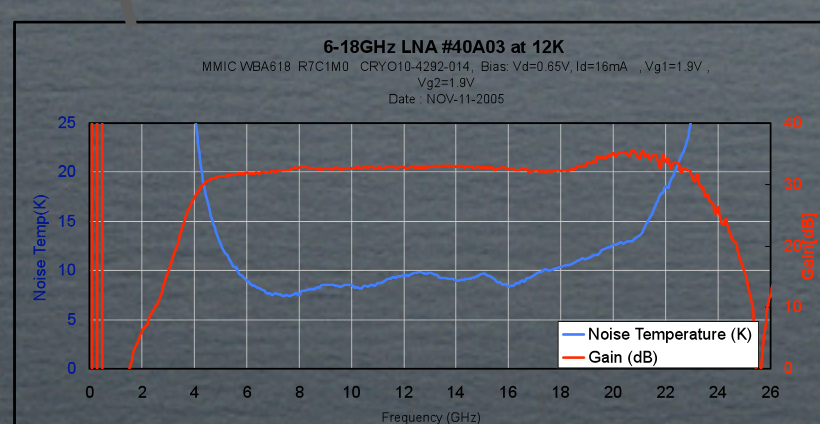

$T_{noise} < 10$ K, 10-18 GHz

BEM rack

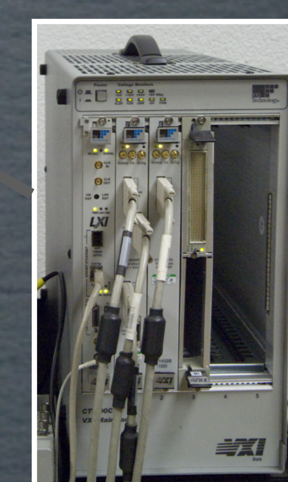

DAE

QUIJOTE Second Instrument

- 16 polarimeters operating at 30 GHz
- Conceptual design re-scaled version of the First Instrument

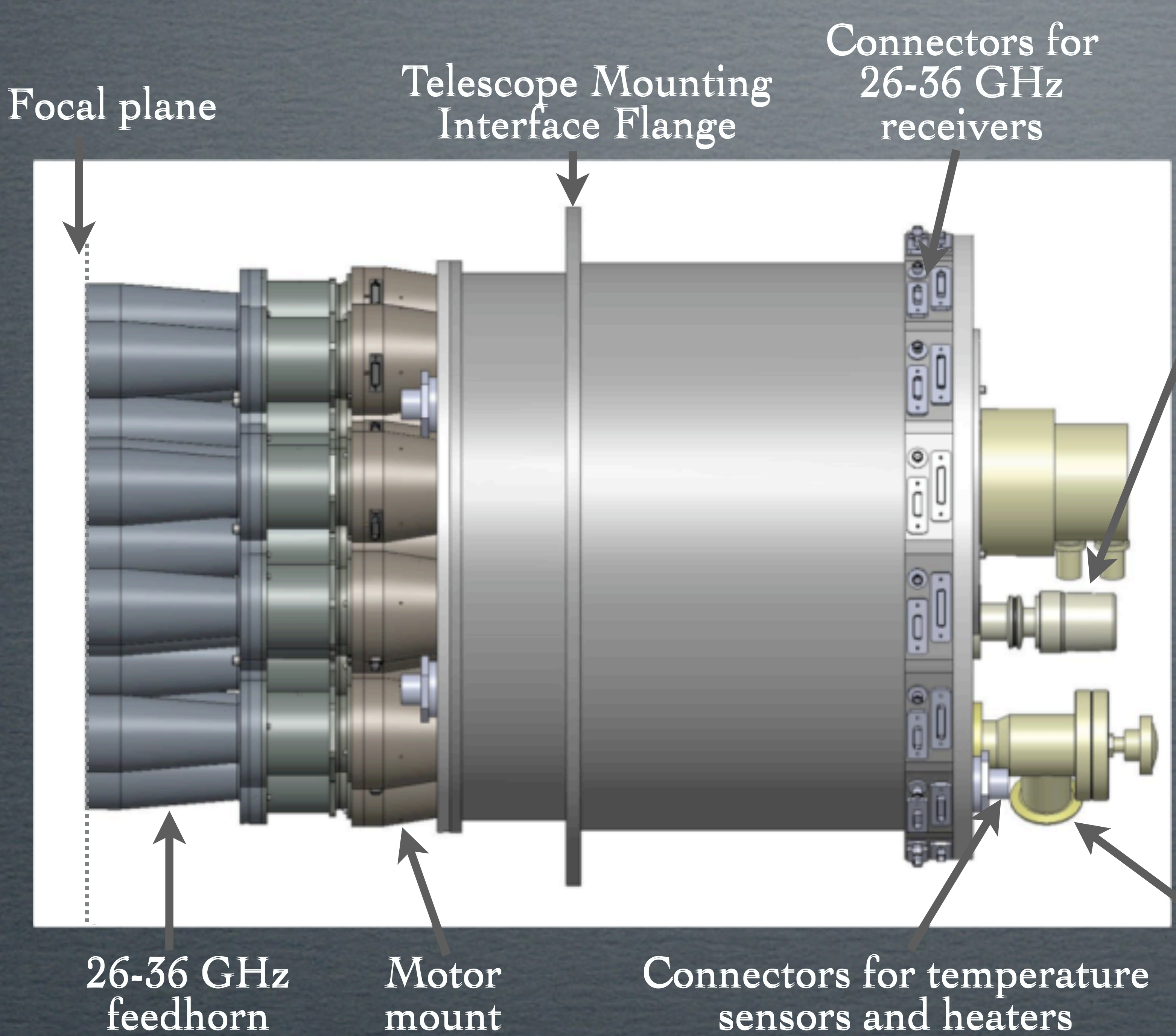

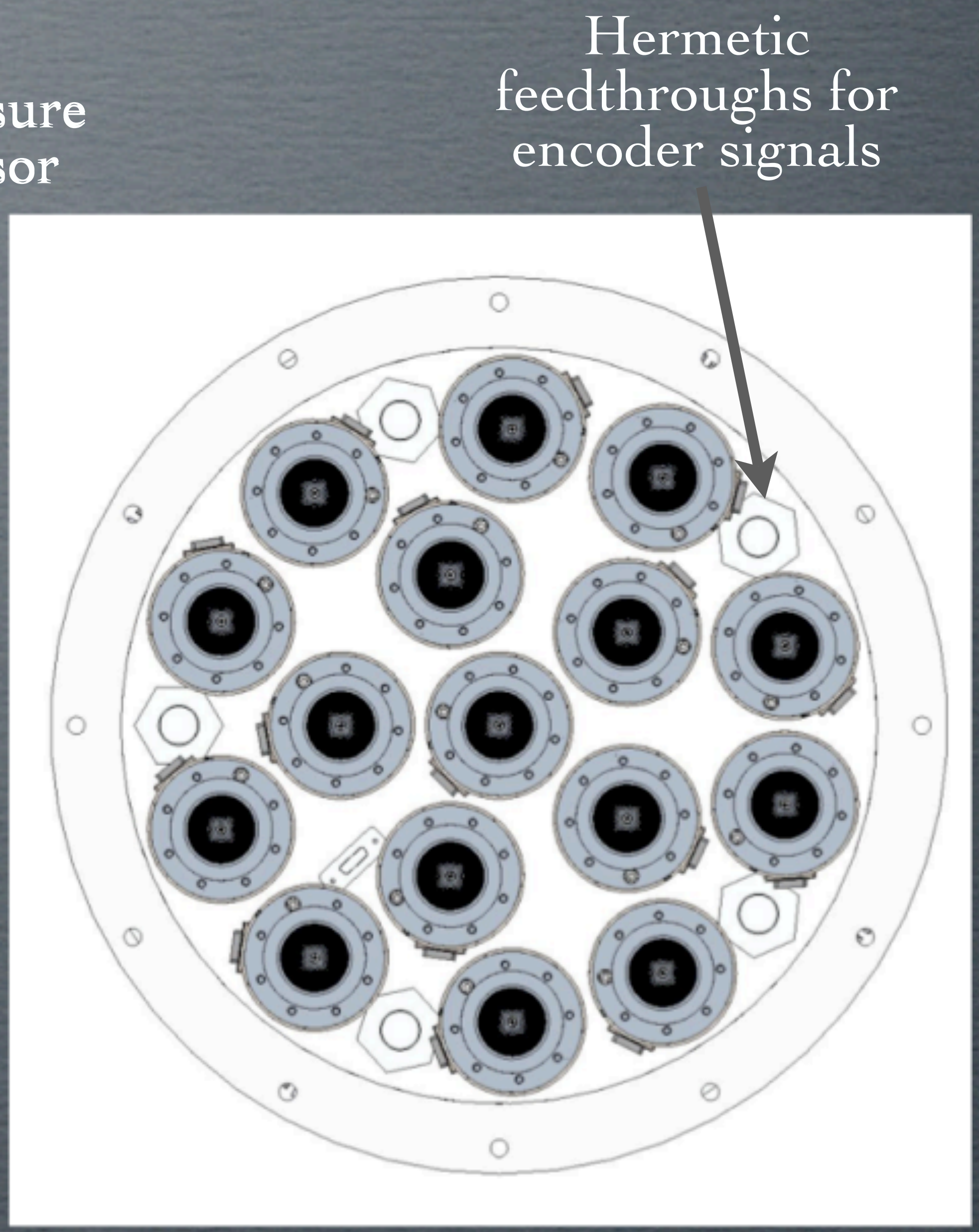

QUIJOTE Second Instrument

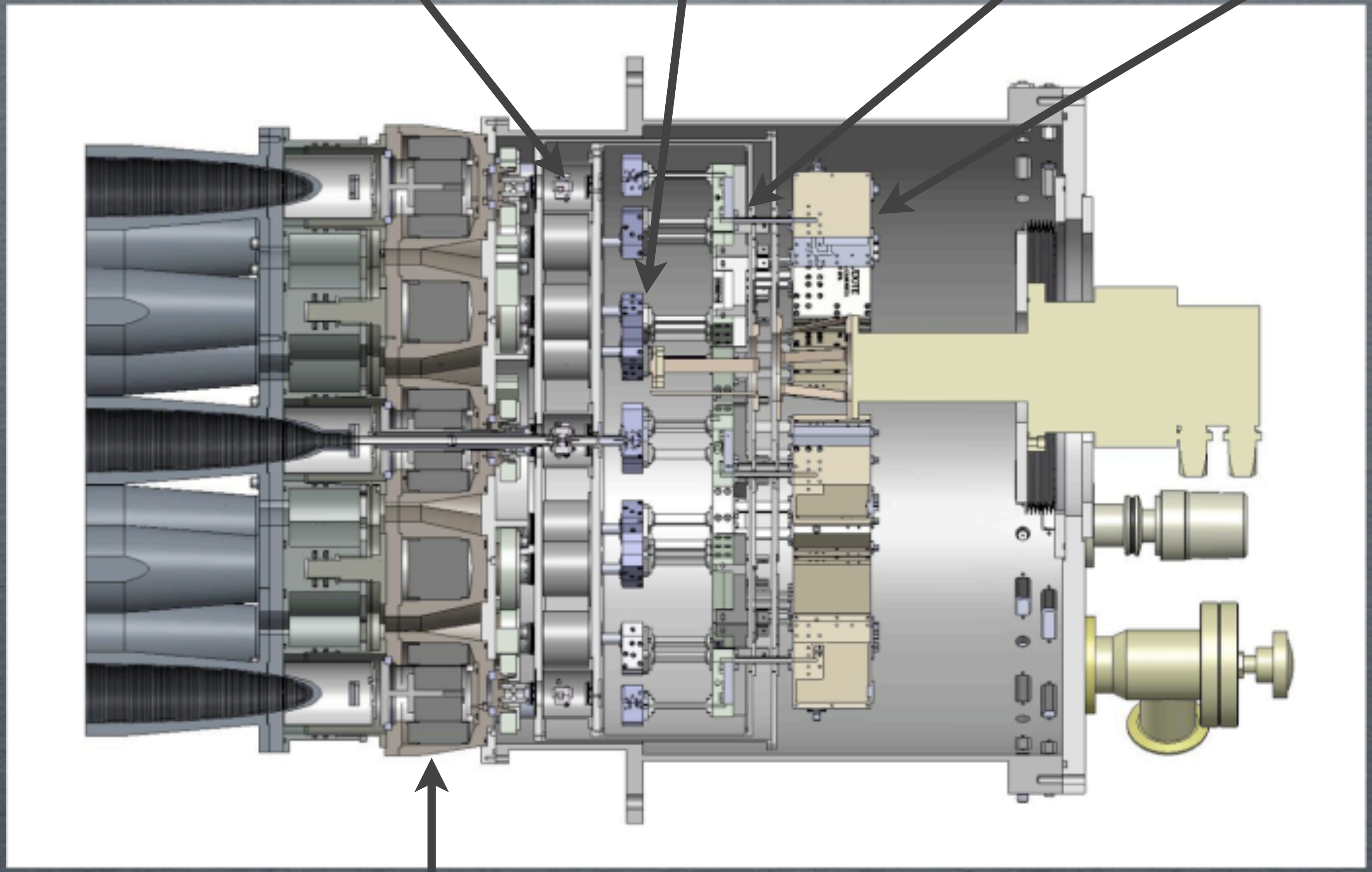

QUIJOTE Instrument characteristics

	1st Ins.					2nd Ins.
Frequency (GHz)	11.0	13.0	17.0	19.0	30.0	30.0
Bandwidth (GHz)	2.0	2.0	2.0	2.0	8.0	8.0
Number of channels	8	8	8	8	2	32
Beam FWHM (deg)	0.92	0.92	0.60	0.60	0.37	0.37
T_{sys} (K)	20.0	20.0	20.0	20.0	30.0	20.0
Sensitivity per beam (Jy $s^{1/2}$)	0.24	0.34	0.24	0.30	0.43	0.08
Sensitivity (mK $s^{1/2}$)	0.22	0.22	0.22	0.22	0.34	0.06

- Sensitivity per beam given by: $$\Delta Q = \Delta U = \sqrt{2}\ \frac{T_{\rm sys}}{\sqrt{\Delta\nu\ t_{\rm int}\ N_{\rm chan}}}$$
- Definition of Q: $Q = T_x - T_y$

QUIJOTE scanning strategy

- Four observing modes:
  - Nominal (first to be implemented): the telescope spins at a fixed elevation with a constant velocity in azimuth. Earth rotation provides a daily sky coverage of several thousands square degrees. Maximum zenith aperture=60º
  - Positioning: stays at a fixed azimuth and elevation
  - Tracking: follows the RA-Dec coordinates of source on the sky
  - Scanning: azimuth scans at a fixed elevation

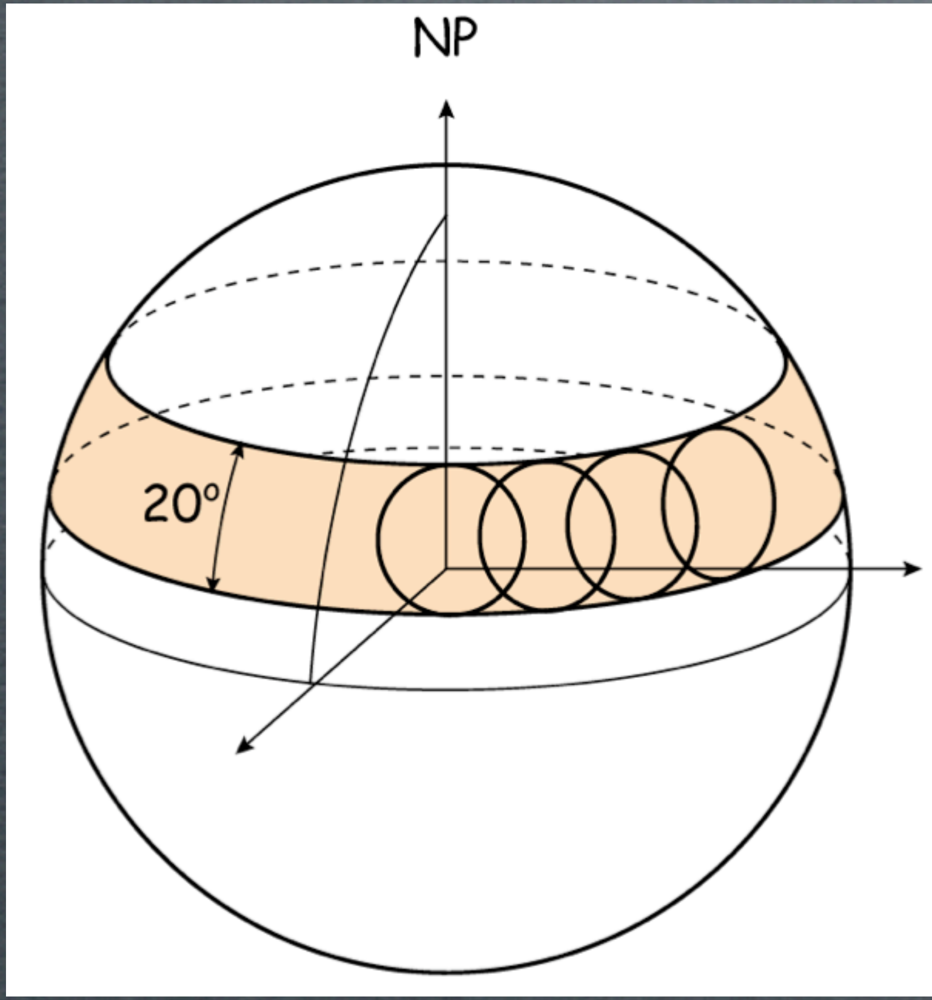

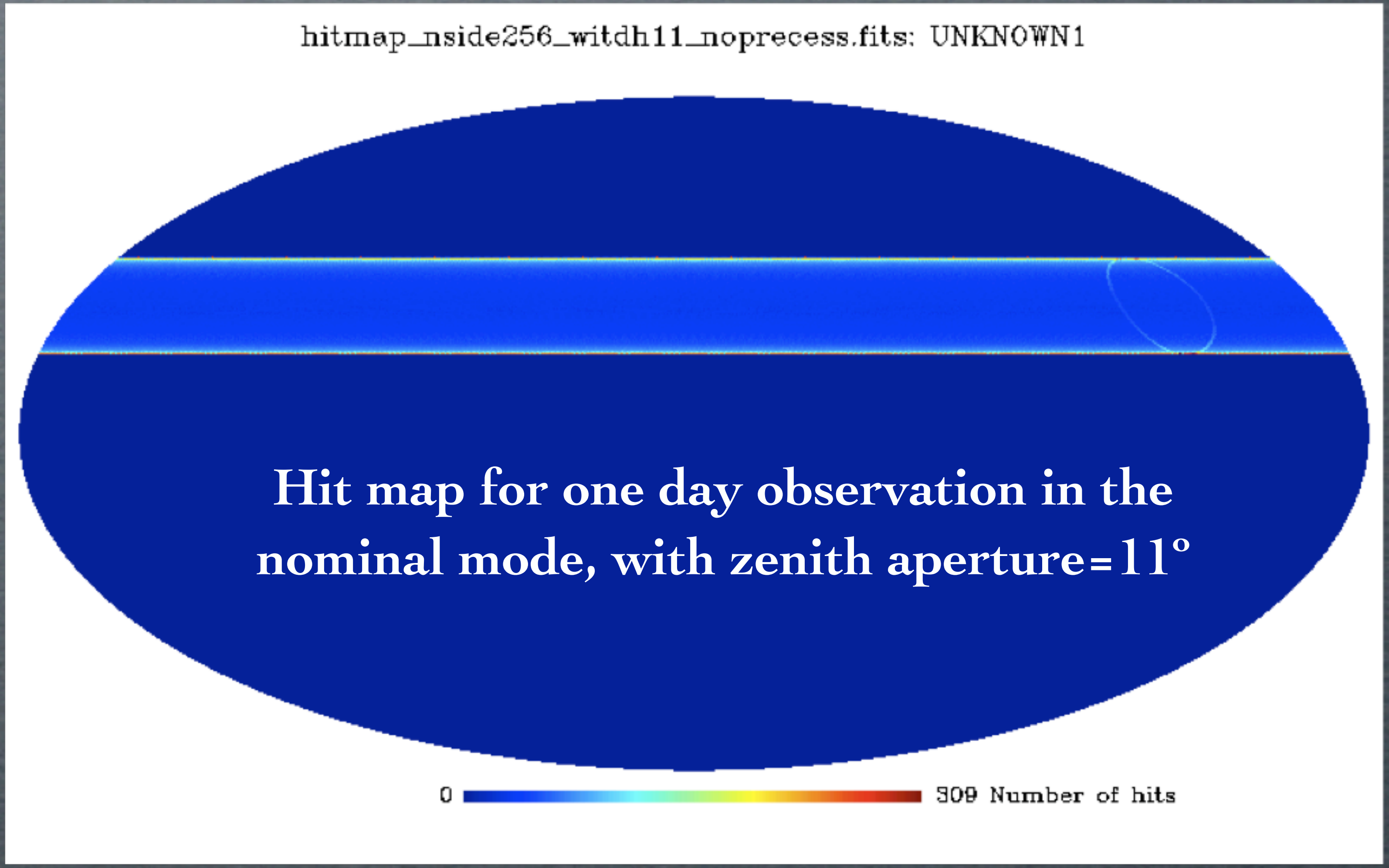

Hit map for one day observation in the nominal mode, with zenith aperture=11º

QUIJOTE Foregrounds Science

❖ Foreground contamination at 30 GHz in comparison with B-modes

- The synchrotron signal (large-dashed lines) corresponds to the total expected contribution in polarization based on La Porta et al. (2006)

- Radio source contribution (short-dashed line) for the cases a population with fluxes in total intensity below:
  - 1 Jy (upper line)
  - 300 mJy (lower line)

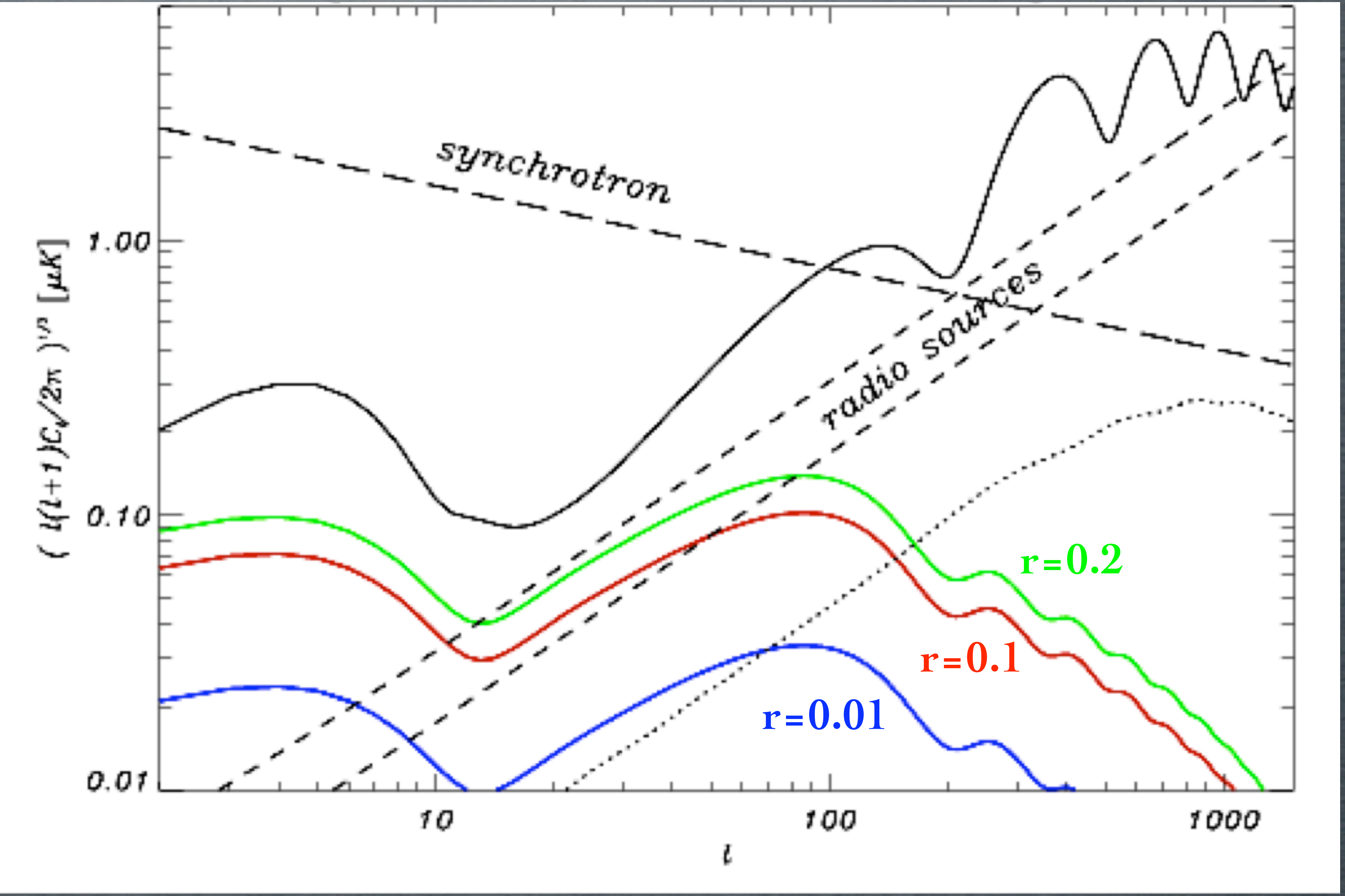

❖ Characterization of the synchrotron emission with the First Instrument

- Instantaneous sensitivity: 0.224 mK $s^{1/2}$
- Effective observation time: 1 year
- Sky coverage: 5000 deg^2

- Effective integration time per 1-degree beam: 1.99 h
- Final map sensitivity: 2.65 μK/beam

- We will obtain four 5000 deg^2 maps of the synchrotron emission at @ 11, 13, 17 and 19 GHz with a sensitivity of ~ 2-3 μK/beam
- Assuming synchrotron frequency dependence as ν^{-3} this will allow to predict the synchrotron contribution at 30 GHz with a precision better than 0.02 μK/beam

- Radio sources: $S_c < 1$ Jy
- Anomalous emission: dust-correlated emission in Cosmosomas (Hildebrandt et al. 2007). ΔT_{rms}=40-80μK @ 11 GHz and 15-30μK @ 15 GHz Polarization: 1%

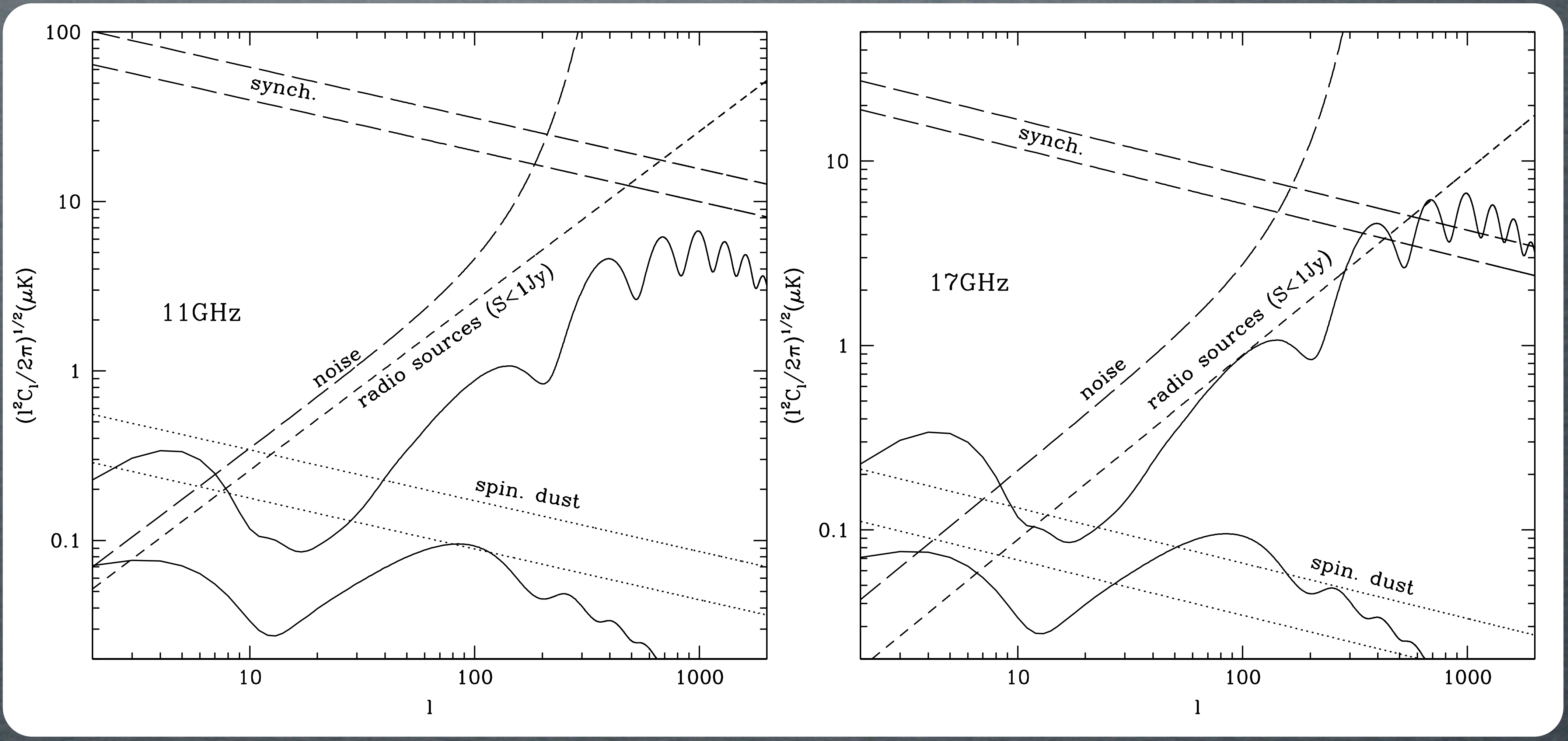

- Noise: 5 μK/beam @ 11 GHz
- Noise: 3 μK/beam @ 17 GHz

❖ Correction of the synchrotron emission at 30 GHz

- The spectral index of the synchrotron emission will be estimated from the First Instrument maps at 10-20 GHz
- Then, assuming a pure power-law dependence, the contribution at 30 GHz is calculated by extrapolation
- A pixel-by-pixel correction is performed of the Second Instrument map at 30 GHz

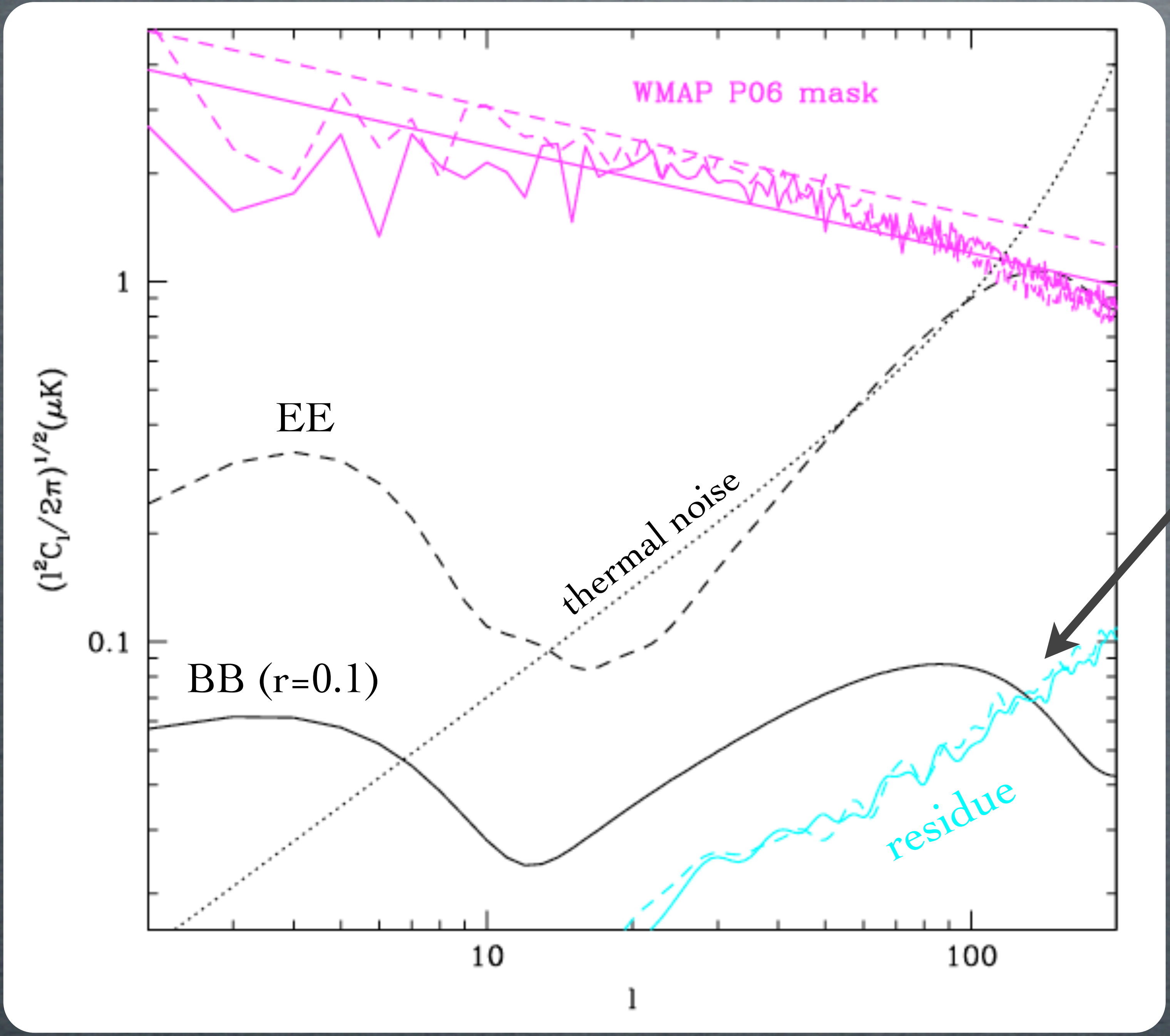

Synchrotron residual contribution at 30 GHz, assuming 2 μK/beam noise in the 10-20 GHz channels

❖ Correction of radio sources at 30 GHz

• Dedicated instrument at 33 GHz. VSA Source Subtractor upgraded for measuring polarization (HWP)

• Twofold subtraction strategy:

- NVSS-GB6 extrapolation. ~250 sources with Stokes-I flux > 300 mJy. Flux sensitivity per source ~2-3 mJy in ~100 days
- Identify sources in the low-frequency channels by MH wavelet filters (López-Caniego et al. 2009)

• Interferometer of two 3.7m antennae with a 9m baseline
• Primary beam: 9'
• Synthesized beam: 4'
• Dec. range: $-5^\circ<\delta<+60^\circ$

❖ Correction of radio sources at 30 GHz

- Power spectrum of polarized radio sources before and after subtraction at 30 GHz:

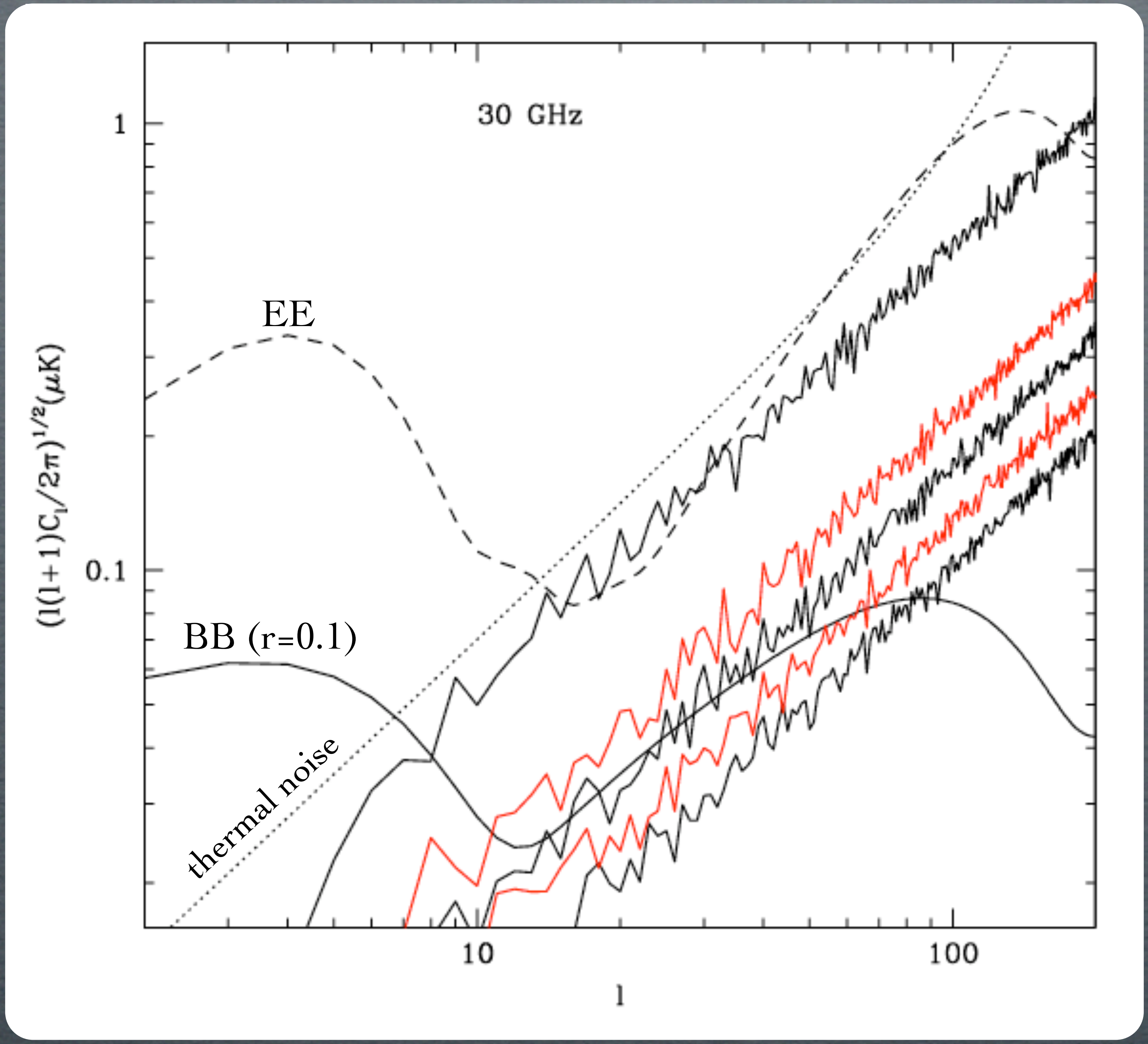

All radio sources

PI < 50 mJy

I < 300 mJy

PI < 10 mJy

I < 100 mJy

QUIJOTE B-mode Science

❖ Second instrument:

- Instantaneous sensitivity: 0.057 mK $s^{1/2}$
- Effective observation time: 3 years
- Sky coverage: 5000 deg^2

- Effective integration time per 1-degree beam: 5.96 h
- Final map sensitivity: 0.38 μK/beam

Predicted performance

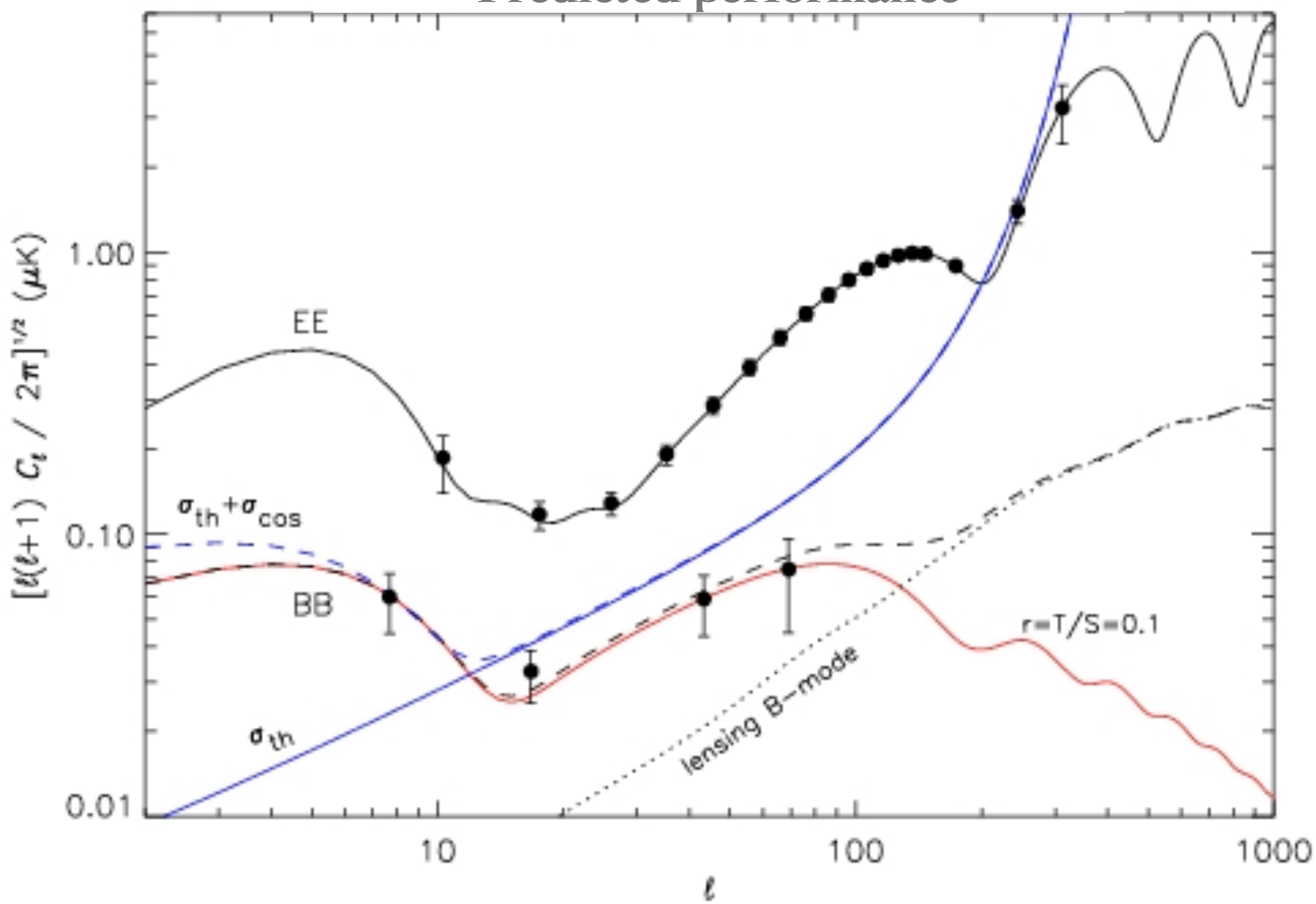

r=0.1 (95% CL) with 5,000 deg^2 sky coverage and 3 years effective observing time

QUIJOTE-CMB Experiment